Pergamon

Geochimica et Cosmochimica Acta, Vol. 67, No. 14, pp. 2663–2681, 2003

0016-7037/03 $30.00 + .00

doi:10.1016/S0016-7037(00)01416-3

Effects of fO_2, fS_2, temperature, and melt composition on Fe-Ni exchange between olivine and sulfide liquid: Implications for natural olivine–sulfide assemblages

JAMES M. BRENAN*

Department of Geology, University of Toronto, Toronto, Canada M5S 3B1

(*Received June* 25, 2002; *accepted in revised form September* 6, 2002)

Abstract—The apparent equilibrium constant for the exchange of Fe and Ni between coexisting olivine and sulfide liquid ($K_D = (X_{NiS}/X_{FeS})_{liquid}/(X_{NiSi12O2}/X_{FeSi12O2})_{olivine}$; X_i = mole fraction) has been measured at controlled oxygen and sulfur fugacities ($fO_2 = 10^{-8.1}$ to 10^{-10} and $fS_2 = 10^{-0.9}$ to $10^{-1.7}$) over the temperature range 1200 to 1385°C, with 5 to 37 wt% Ni and 7 to 18 wt% Cu in the sulfide liquid. At log fO_2 of -8.7 ± 0.1, and log fS_2 of -0.9 to -1.7, K_D is relatively insensitive to sulfur fugacity, but comparison with previous results shows that K_D increases at very low sulfur fugacities. K_D values show an increase with the nickel content of the sulfide liquid, but this effect is more complex than found previously, and is greatest at log fO_2 of -8.1, lessens with decreasing fO_2, and K_D becomes independent of melt Ni content at log $fO_2 \leq -9.5$. The origin of this variation in K_D with fO_2 and fS_2 is most likely the result of nonideal mixing of Fe and Ni species in the sulfide liquid. Such behavior causes activity coefficients to change with either melt oxygen content or metal/sulfur ratio, effects that are well documented for metal-rich sulfide melts.

Application of these experimental results to natural samples shows that the relatively large dispersion that exists in K_D values from different olivine + sulfide-saturated rock suites can be interpreted as arising from variations in fO_2, fS_2, and the nickel content of the sulfide liquid. Estimates of fO_2 based on K_D and sulfide melt composition in natural samples yields a range from fayalite–magnetite–quartz (FMQ)–1 to FMQ-2 or lower, which is in good agreement with previous values determined for oceanic basalts that use glass ferric/ferrous ratios. Anomalously high K_D values recorded in some suites, such as Disko Island, probably reflect low fS_2 during sulfide saturation, which is consistent with indications of low fO_2 for those samples. It is concluded that the variation in K_D values from natural samples reflects olivine–sulfide melt equilibrium at conditions within the T-fO_2-fS_2 range of terrestrial mafic magmas. *Copyright © 2003 Elsevier Science Ltd*

1. INTRODUCTION

Numerous studies have used nickel partitioning between olivine and sulfide liquid to assess the magmatic nature of both base metal sulfide segregations associated with mafic and ultramafic plutonic rocks (Boctor, 1981, 1982; Fleet and MacRae, 1983, 1987; Thompson, et al., 1984; Barnes and Naldrett, 1985) and sulfide inclusions hosted by phenocrysts in mafic lavas (Fleet et al., 1977, 1981; Pederson, 1979; Fleet and Stone, 1990). The reaction that describes the partitioning of nickel between olivine and an iron and sulfur-rich, oxygen-poor liquid can be expressed as

$$FeS_{(liquid)} + NiSi_{1/2}O_{2(olivine)} \Leftrightarrow NiS_{(liquid)} + FeSi_{1/2}O_{2(olivine)} \quad (1)$$

where $FeS_{(liquid)}$ and $NiS_{(liquid)}$ refer to hypothetical species in the sulfide melt and $NiSi_{1/2}O_{2(olivine)}$, $FeSi_{1/2}O_{2(olivine)}$ are the appropriate components in the olivine solid solution. With the assumption of ideal mixing of all components, the equilibrium constant for Eqn. 1 is often expressed as an exchange coefficient, K_D, taking the form

$$K_D = (X_{NiS}/X_{FeS})_{liquid}/(X_{NiSi1/2O2}/X_{FeSi1/2O2})_{olivine} \quad (2)$$

where X_i is equal to the mole fraction of component i in the phase of interest. Values of K_D have been measured experimentally (i.e., Clark and Naldrett, 1972; Fleet et al., 1977, 1981; Boctor, 1981, 1982; Fleet and MacRae, 1983, 1987; Fleet and Stone, 1990; Gaetani and Grove, 1997; Brenan and Caciagli, 2000) or estimated by the compositions of naturally occurring olivine and coexisting sulfide (Fleet et al., 1977; Thompson, 1982, 1984; Barnes and Naldrett, 1985; Fleet and Stone, 1990). K_D values recorded by natural samples often differ significantly from those determined by experiment, which has been used to suggest that natural sulfide–olivine assemblages do not represent high-temperature equilibrium, thus calling into question their magmatic origin (e.g., Fleet and MacRae, 1983; Fleet and Stone, 1990). However, Brenan and Caciagli (2000) determined that K_D is a function of both fO_2 and melt Ni content and that the variation in K_D recorded by natural samples can be reconciled in terms of changes in both these parameters at the magmatic stage. Fleet and MacRae (1983) and more recently Fleet (2001) have argued that at a given fO_2 and fS_2, K_D is unaffected by sulfide melt composition and that any variation in K_D, such as that observed by Brenan and Caciagli (2000), is a consequence of the failure to achieve equilibrium. In this contribution, the results of additional measurements of K_D are presented, including tightly bracketed reversal experiments, and the effects of fO_2, fS_2, temperature, and melt composition (Ni, Cu, and O content) are explicitly addressed. With this comprehensive data set, it is shown that the variation in K_D with melt Ni content, as originally documented by Brenan and Caciagli (2000), is robust. However, the magnitude of this effect is found to diminish with decreasing

* Author to whom correspondence should be addressed (brenan@geology.utoronto.ca).

fO_2, which possibly explains the differences between previously published data sets.

2. EXPERIMENTAL AND ANALYTICAL METHODS

Experiments were conducted in a modified 1-atm vertical tube furnace with mixtures of CO, CO_2, and SO_2 gases to control oxygen and sulfur fugacity; the furnace design is similar to that described in Brenan and Caciagli (2000). Experiments of this study were performed at log fO_2 ranging from −8.1 to −10.1, and log fS_2 from −0.9 to −1.7, and a summary of these experiments, along with those performed by Brenan and Caciagli (2000), is provided in Table 1. Note that there is a small shift in fO_2 and fS_2 values listed in Table 1 compared with those originally published in Brenan and Caciagli (2000). This is the result of a small change in the flow-rate calibration and an error in the input data (JANAF tables) for the free energy of formation (G_f) of the gas species S_2O, H_2S_2 and HS (V. Kress, personal communication) used in these previous calculations. A revised version of the program COHSmix, supplied by Victor Kress, was used to calculate the values of fO_2 and fS_2 in this article. The accuracy of quoted sulfur fugacity was assessed by the pyrrhotite sulfur barometer of Toulmin and Barton (1964) at 900°C and log fS_2 of −1.5, −2, and −3 and by determining the fS_2 of the Ru-RuS_2 equilibrium at 1200°C. Oxygen fugacity was checked using the stability of solid oxide buffers (nickel–nickel oxide, molybdenum–molybdenum oxide, iron–wüstite), and we have also employed the NiO-Pd redox sensor at 1000°C (Pownceby and O'Neill, 1994). On the basis of this assessment, we estimate fS_2 and fO_2 accuracy to be within 0.3 log units.

Sulfide melt was added to experiments as mixtures of pure metal and elemental sulfur, weighed and ground to the desired proportions. A typical experiment contained this metal–sulfur mix (hereafter referred to as sulfide melt), San Carlos olivine (powdered to pass 400 mesh; ≤40 μm), and with the exception of experiments MF1a and b, powdered synthetic basalt glass (modeled after the 401 diabase of Roeder and Reynolds, 1996), all within crucibles fabricated from San Carlos olivine megacrysts. Some experiments also used a powdered oxide mix with forsterite stoichiometry in lieu of San Carlos olivine. We assessed the inertness of the olivine crucibles by considering the effect of the crucible on changing the composition of its contents over the course of an experiment. As a result of to the relatively low rate of Fe-Ni interdiffusion within the crucible (Brenan and Caciagli, 2000) combined with the incompatibility of Fe and Ni in olivine relative to sulfide liquid, changes in sample composition as a result of exchange with the crucible are negligible.

Approximately 25 mg of the olivine–two-melt mixture were loaded into a crucible, in proportions of 20% olivine, 60% sulfide melt, and 20% silicate melt. Holders for the olivine crucibles were fabricated from silica rod and cylinders cut from silica tubing; up to four olivine crucibles could be run simultaneously in this configuration (see fig. 2 of Andrews and Brenan, 2002). Sample holders were suspended from a hook fashioned at the end of a ~60-cm-long × 3-mm-diameter silica rod. In a typical experiment, the silica rod was retracted so that the loaded sample holder was initially positioned in the upper cool region of the furnace. The furnace was then sealed and gas flow initiated. After 20 to 30 min, the rod was lowered to position the holder within the predetermined furnace hot spot, where samples remained for 3 to 5 d. Samples were quenched by rapid immersion in a cold water bath situated outside the lower end of the furnace tube.

Run products were extracted from their olivine crucible, then mounted in epoxy, polished, and carbon-coated in preparation for textural and electron microprobe analysis. As documented by Fleet and MacRae (1983), the nickel content of olivine immersed in a Ni-rich sulfide melt can be overestimated as a result of Ni X-ray fluorescence from the sulfide melt. To avoid this problem, the two samples that were run with olivine + sulfide melt (MF1a and 1b) were first coarsely crushed, some melt-bearing fragments set aside, and the rest cleaned in warm aqua regia to dissolve the sulfide melt and produce a clean olivine separate (after the method of Fleet and MacRae, 1983). Sample fragments and clean olivine separates were then mounted and prepared as per other experiments. For the case of experiments containing silicate and sulfide melt, olivine grains were always completely immersed in silicate melt (Fig. 1), and this cleaning procedure was deemed unnecessary.

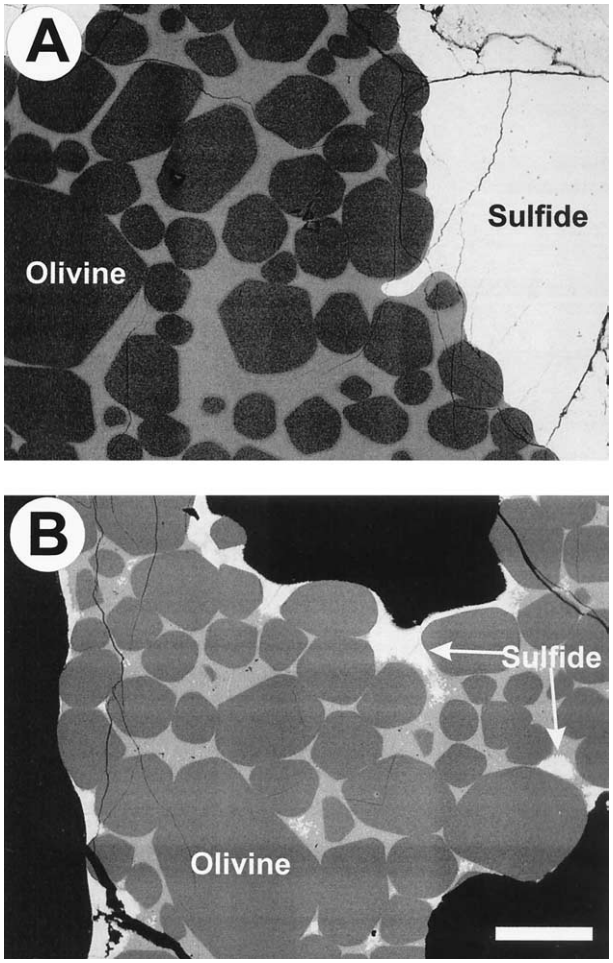

Fig. 1. Backscattered electron images of representative run products from experiments performed at 1300°C. Olivine (dark gray) and sulfide (white) are as indicated, and the light gray material surrounding olivine is quenched silicate melt. (A) Product from experiment MF9b, log fO_2 = −8.7, log fS_2 = −0.9, 5.5 wt% Ni in the sulfide melt. (B) Product from experiment MF5a, log fO_2 = −8.2, log fS_2 = −1.7, 11.5 wt% Ni in the sulfide melt. The scale bar in (B) is 100 μm and refers to both images.

All run-product phases were analyzed with the Cameca SX50 electron microprobe at the University of Toronto. Analyses were conducted with an accelerating voltage of 20 kV and a beam current of 30 nA on sulfide melt and 50 nA on olivine, with on-peak counting times of 20 s for major elements and 60 s for nickel in olivine and oxygen in sulfide melt. A focused spot was used for olivine analyses, and a 30-μm diameter defocused beam was used to analyze the quenched sulfide melt. Standards for sulfide melt analysis were pentlandite (Fe, S, Ni), chalcopyrite (Cu) and hematite (O). Oxygen was analyzed with an ODPB pseudocrystal, and the hematite standard was carbon-coated at the same time as the unknowns to minimize inaccuracies due to the effects of coat thickness on oxygen X-ray attenuation. Standards for olivine analysis were synthetic olivine (Si, Mg, Fe), bustamite (Ca, Mn), and pentlandite (Ni). Raw count rates were converted to concentrations with a modified ZAF correction routine. Summaries of olivine and sulfide liquid compositions are provided in Tables 2 and 3, respectively.

3. RESULTS AND DISCUSSION

3.1. Textural Observations

Examples of the mutual textural relations among coexisting run-product phases are provided in Figure 1. Olivines are

Table 1. Summary of Experiments

Run ID[1]	days	T (°C)	type	$CO:SO_2:CO^2$	Fe-Ni-Cu-S[6]	log fO_2	log fS_2	K_D[7]	wt% Ni
D.0l-1	1	1300	sulf melt only	35:28:100	40-30-0-30	−8.2	−1.7	27.7 (6.5)	32.6 (6.0)
D.ol-2	1	1400	sulf melt only	39:08:55	40-30-0-30	−8	−1.8	24.4 (2.7)	28.3 (2.2)
D.ol-3	3	1300	sulf melt only	35:28:100	40-30-0-30	−8.2	−1.7	29.7 (5.3)	31.4 (4.6)
D.ol-5	4.5	1200	sulf melt only	28:56:00	40-30-0-30	−8.7	−1.1	24.5 (5.6)	31.2 (5.5)
D.ol-7	2	1300	sulf melt only	35:28:100	55-15-0-30	−8.2	−1.7	19.4 (5.1)	22.1 (5.1)
D.ol-8	3	1200	sulf melt only	28:56:00	55-15-0-30	−8.7	−1.1	12.9 (1.1)	13.8 (2.5)
D.ol-9	2	1300	sulf melt only	71:23:182	40-30-0-30	−8.6	−1.9	30.0 (4.4)	32.0 (2.3)
D.ol-10	2	1300	sulf melt only	71:23:182	65-6-0-30	−8.6	−1.9	8.2 (4.8)	5.4 (2.6)
D.ol-11	2	1300	sulf melt only	66:8:53	65-5-0-30	−9.5	−1.6	22.4 (7.4)	4.7 (0.6)
D.ol-13	5	1300	sulf melt only	48:12:93	40-30-0-30	−8.8	−1.7	38.0 (6.6)	30.3 (4.4)
D.ol-14	5	1300	sulf melt only	66:8:53	55-15-0-30	−9.5	−1.6	30.8 (4.4)	11.4 (1.5)
D.ol-15	7	1300	sulf melt only	48:12:93	55-15-0-30	−8.8	−1.7	23.9 (5.7)	14.4 (2.8)
D.ol-20	5	1300	sulf melt only	66:8:53	65-5-0-30	−9.5	−1.6	17.3 (8.7)	5.4 (0.8)
D.ol-21	5	1300	sulf melt only (Fo)	48:12:93	40-30-0-30	−8.8	−1.7	22.6 (6.7)	30.8 (4.3)
D.ol-22	5	1300	sulf melt only (Fo)	66:8:53	55-15-0-30	−9.5	−1.6	23.4 (5.8)	13.9 (2.1)
D.ol-23	4	1300	sulf melt only	66:8:53	40-30-0-30	−8.6	−4.1	73.3 (9.5)	52.3 (1.7)
MF1a	8	1300	rev[3]	48:12:93	65-5-0-30	−8.8	−1.7	15.6 (4.8)	5.2 (1.2)
MF1b	8	1300	rev (Fo)[4]	48:12:93	65-6-0-30	−8.8	−1.7	13.8 (4.1)	5.1 (1.2)
MF2a	5	1300	sil + sulf melt[5]	48:12:93	45-25-0-30	−8.8	−1.7	29.9 (3.9)	25.6 (2.8)
MF2b	5	1300	sil + sulf melt	48:12:93	65-5-0-30	−8.8	−1.7	18.6 (2.8)	6.1 (0.8)
MF3a	5	1300	sil + sulf melt	35:28:100	45-25-0-30	−8.2	−1.7	33.8 (3.4)	36.6 (2.6)
MF3b	5	1300	sil + sulf melt	35:28:100	65-5-0-30	−8.2	−1.7	28.1 (4.4)	31 (3.9)
MF4a	5	1300	sil + sulf melt	66:8:53	65-5-0-30	−9.5	−1.6	28.7 (6.2)	4.4 (0.3)
MF4b	5	1300	sil + sulf melt	66:8:53	45-25-0-30	−9.5	−1.6	30.4 (3.9)	22.9 (2.1)
MF5a	5	1300	sil + sulf melt	35:28:100	65-5-0-30	−8.2	−1.7	11.6 (1.5)	11.5 (1.4)
MF5b	5	1300	sil + sulf melt	35:28:100	55-15-0-30	−8.2	−1.7	17.1 (1.5)	18.3 (2.9)
MF6	5	1300	sil + sulf melt	66:8:53	55-15-0-30	−9.5	−1.6	33.2 (4.2)	13.8 (1.4)
MF8a	5	1300	sil + sulf melt	115:17:17	55-15-0-30	−10.1	−1.3	27.2 (5)	13.3 (2.3)
MF8b	5	1300	sil + sulf melt	115:17:17	45-25-0-30	−10.1	−1.3	32 (3.1)	21.9 (1.8)
MF8c	5	1300	sil + sulf melt	115:17:17	65-6-0-30	−10.1	−1.3	32 (7.5)	5.9 (0.5)
MF9a	5	1300	sil + sulf melt	32:17:0	55-15-0-30	−8.7	−0.9	21.9 (2.3)	16.3 (1.5)
MF9b	5	1300	sil + sulf melt	32:17:0	65-5-0-30	−8.7	−0.9	13.7 (1)	5.5 (0.2)
MF9c	5	1300	sil + sulf melt	32:17:0	45-25-0-30	−8.7	−0.9	28.8 (2.3)	25 (1.2)
MF11a	5	1300	sil + sulf melt	27:33:11	65-5-0-30	−8.1	−1.1	9.3 (1.2)	10.8 (1.3)
MF11b	5	1300	sil + sulf melt	27:33:11	55-15-0-30	−8.1	−1.1	15.4 (2.4)	18 (2.7)
MF11c	5	1300	sil + sulf melt	27:33:11	45-25-0-30	−8.1	−1.1	23 (1.5)	28.3 (1.5)
MF13a	5	1200	sil + sulf melt	9:8:20	45-25-0-30	−9.1	−1.4	32.7 (3.4)	29.4 (2.4)
MF13b	5	1200	sil + sulf melt	9:8:20	65-5-0-30	−9.1	−1.4	26.5 (5.2)	19.2 (3.5)
MF13c	5	1200	sil + sulf melt (Fo)	9:8:20	65-5-0-30	−9.1	−1.4	12.7 (3.2)	7.8 (1.9)
MF14a	5	1200	sil + sulf melt	20:5:29	45-25-0-30	−10	−1.5	26.5 (2.6)	24.3 (1.1)
MF14b	5	1200	sil + sulf melt	20:5:29	65-5-0-30	−10	−1.5	22.6 (4.6)	5.4 (0.8)
MF15a	3	1385	sil + sulf melt	23:8:0	65-6-0-30	−8.5	−0.9	11 (1.9)	5.3 (0.9)
MF15b	3	1385	sil + sulf melt (Fo)	23:8:0	65-5-0-30	−8.5	−0.9	17.8 (3.9)	11.6 (2.5)
MF15c	3	1385	sil + sulf melt	23:8:0	45-25-0-30	−8.5	−0.9	30.6 (3.7)	32.1 (3.1)
MF16a	5	1300	sil + sulf melt	48:12:93	60-5-5-30	−8.8	−1.7	22.8 (3.3)	7.4 (1)
MF16b	5	1300	sil + sulf melt	48:12:93	50-5-15-30	−8.8	−1.7	22.2 (2.5)	6 (0.5)
MF16c	5	1300	sil + sulf melt	48:12:93	40-15-15-30	−8.8	−1.7	26 (1)	17.3 (0.2)
MF17a	3	1385	sil + sulf melt	32:8:0	65-5-0-30	−8.9	−1	25.3 (4.6)	5.5 (0.3)
MF17b	3	1385	sil + sulf melt (Fo)	32:8:0	65-5-0-30	−8.9	−1	24.4 (4.0)	4.4 (0.3)
MF17c	3	1385	sil + sulf melt	32:8:0	45-25-0-30	−8.9	−1	27.1 (3.4)	21.9 (2.4)

Notes:
[1]Samples with the same number prefix were run together.
[2]Refers to gas flow rates in cm^3/minute.
[3]rev: reversal experiment, sample run for 4 days, quenched, finely powdered, run for additional 4 days.
[4](Fo): olivine component was added as powdered oxide mix of forsterite stoichiometry, all other experiments used powdered San Carlos olivine.
[5]sil melt: experiment contained ~10 wt% basaltic melt added with sulfide melt.
[6]Initial weight ratio of metals and sulfur added as "sulfide melt".
[7]molar ratio of $(Fe/Ni)_{olivine}$/(Fe/Ni)sulfide liquid.

relatively large (100 μm or more) compared with the starting grain size (≤40 μm), have developed sub- to euhedral shapes, and are always preferentially wetted by silicate melt. In the presence of silicate melt, molten sulfide occurs as isolated globules, with more extensive coalescence of globules occurring in experiments at lower fO_2 (cf. Figs. 1A and 1B). Relative to the experiments that contained only sulfide melt, olivines in runs with both silicate and sulfide melt have undergone significantly more coarsening, presumably as a result of the high solubility of olivine components in the silicate melt. Sulfide melt quenches to an intergrowth of primarily Fe-Ni sulfide (MSS, pyrrhotite), except in runs at the highest fO_2 and lowest Ni content, in which several volume percent of quench Fe-oxide dendrites were also observed.

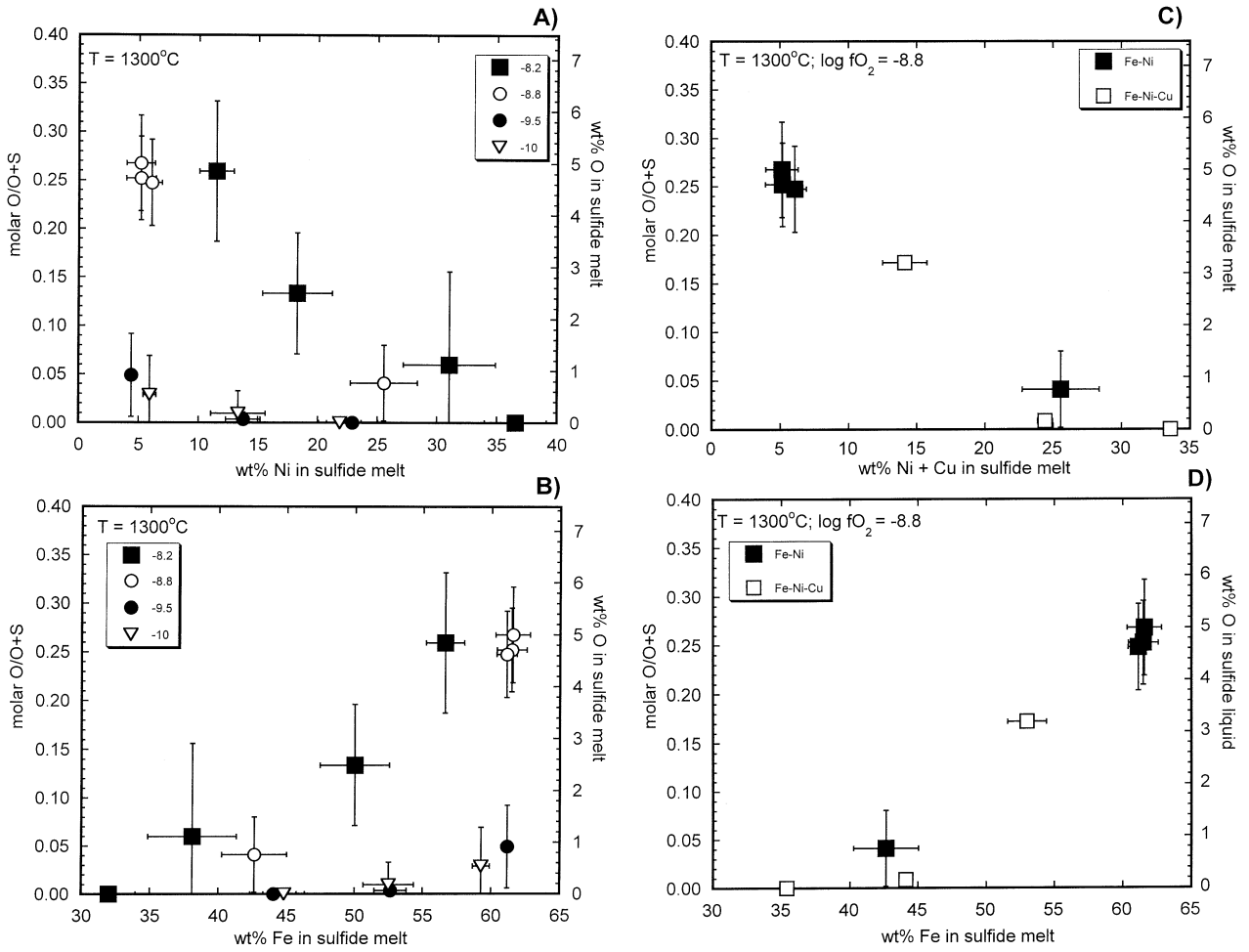

Fig. 2. Molar O/O + S ratio and oxygen content of sulfide melt as a function of melt Ni (± Cu) and Fe contents. Data are from experiments performed at 1300°C, log fS_2 −1.7 ± 0.1 and at the log fO_2 values indicated. Values portrayed in (A) and (B) are from experiments performed with Cu-free melts, whereas (C) and (D) compare data for Cu-bearing experiments.

3.2 Phase Compositions

Olivines produced in experiments are compositionally homogeneous, as judged by microprobe scans across single grains and the small standard deviation of multiple grain analyses (Table 2). Olivines also exhibit a compositional shift with respect to either the forsterite oxide mix or San Carlos olivine (SCO) used as starting materials (the latter has 48.77 ± 0.81 wt% MgO, 9.5 ± 1.04 wt% FeO, 0.38 ± 0.04 wt% NiO; table 2 of Brenan and Caciagli, 2000). The most significant change occurs for the olivines produced in silicate melt–bearing experiments, in which the abundances of Fe and Ni may increase by up to threefold (e.g., MF13a, b; Table 2), with Mg levels decreasing in accord with charge balance.

In most experiments, the Fe and Ni content of the sulfide melt was found to be similar to that initially added to the experiment, but in a few instances, melt Ni abundances increased significantly, with a corresponding reduction in Fe. Experiments run at the highest fO_2 exhibit this behavior and show textural evidence for loss of sulfide melt to the silica sample holder, which is a consequence of the enhanced wetting of molten sulfide against olivine at high fO_2 (e.g., Rose and Brenan, 2001). The increased Ni content of sulfide melts from those experiments results from a decreased mass fraction of this phase within the olivine crucible, thus increasing the sulfide Ni content, as dictated by both mass balance and the higher sulfide/silicate melt partition coefficient for Ni relative to Fe (Peach and Mathez, 1993). As a result of the low viscosity of sulfide melt, it is likely that melt escape occurred at the initial stages of experiments, and that phase proportions were constant for most of the experiment duration. Olivines from experiments that experienced sulfide melt loss are homogeneous, and values of K_D are consistent with those obtained from samples that had high Ni abundances initially. As such, experiments that experienced sulfide melt loss are considered to be equilibrated and are included in the data set discussed below.

As a result of to the very low viscosity of molten sulfide, it was not possible to cool samples rapidly enough to form a glass (although coexisting silicate melts did form glasses), and thus the composition of sulfide liquids produced in experiments may have been modified during the quenching process. Splat

Table 2. Summary of olivine analyses (wt%)

Sample	n	SiO_2[1]	MgO	MnO	FeO	CaO	NiO[2]	Total
MF1a	26	40.23 (0.15)	46.97 (0.17)	0.052 (0.013)	12.94 (0.11)	0.065 (0.01)	0.069 (0.013)	100.32
MF1b	26	40.49 (0.2)	48.61 (0.46)	0.019 (0.015)	10.53 (0.72)	0.072 (0.012)	0.063 (0.011)	99.78
MF2a	26	38.87 (0.17)	40.93 (0.22)	0.082 (0.014)	19.63 (0.08)	0.238 (0.012)	0.39 (0.014)	100.15
MF2b	20	38.28 (0.17)	39.07 (0.21)	0.071 (0.016)	22 (0.12)	0.284 (0.017)	0.116 (0.006)	99.82
MF3a	20	38.04 (0.26)	37.61 (0.25)	0.069 (0.015)	23.18 (0.13)	0.375 (0.015)	0.774 (0.029	100.05
MF3b	20	37.97 (0.35)	36.85 (0.37)	0.072 (0.012)	24.42 (0.09)	0.402 (0.026)	0.7 (0.025)	100.42
MF4a	25	40.26 (0.26)	47.02 (0.31)	0.052 (0.013)	12.12 (0.07)	0.167 (0.018)	0.031 (0.006)	99.65
MF4b	24	40.84 (0.24)	48.24 (0.31)	0.09 (0.006)	9.93 (0.05)	0.127 (0.008)	0.162 (0.017)	99.12
MF5a	18	38.23 (0.25)	37.27 (0.2)	0.071 (0.015)	24.41 (0.1)	0.498 (0.022)	0.422 (0.008)	100.91
MF5b	10	38.15 (0.14)	37.10 (0.17)	0.082 (0.011)	24.36 (0.08)	0.46 (0.029)	0.516 (0.013)	100.67
MF6	20	40.48 (0.26)	47.74 (0.27)	0.062 (0.009)	11.65 (0.06)	0.153 (0.011)	0.091 (0.006)	100.18
MF8a	5	40.65 (0.12)	49.29 (0.17)	0.062 (0.003)	9.17 (0.06)	0.147 (0.005)	0.085 (0.005)	99.41
MF8b	5	40.9 (0.13)	49.87 (0.13)	0.07 (0.012)	8.39 (0.08)	0.148 (0.01)	0.127 (0.005)	99.5
MF8c	5	40.49 (0.02)	47.99 (0.05)	0.046 (0.008)	11.59 (0.04)	0.139 (0.006)	0.036 (0.008)	100.29
MF9a	10	38.8 (0.17)	40.4 (0.89)	0.077 (0.01)	20.28 (0.24)	0.341 (0.302)	0.298 (0.014)	100.2
MF9b	10	38.46 (0.11	39.75 (0.2)	0.066 (0.009)	21.52 (0.05)	0.259 (0.013)	0.137 (0.008)	100.2
MF9c	10	38.78 (0.13)	40.98 (0.19)	0.086 (0.006)	19.44 (0.09)	0.207 (0.01)	0.397 (0.022)	99.89
MF11a	14	37.89 (0.15)	36.86 (0.15)	0.075 (0.009)	25.15 (0.15)	0.478 (0.018)	0.504 (0.011)	100.96
MF11b	15	37.84 (0.1)	36.67 (0.09)	0.074 (0.01)	25.44 (0.09)	0.45 (0.028)	0.59 (0.012)	101.07
MF11c	14	37.86 (0.33)	36.85 (0.38)	0.076 (0.01)	24.93 (0.16)	0.406 (0.017)	0.749 (0.013)	100.87
MF13a	15	36.82 (0.13)	32.22 (0.14)	0.069 (0.007)	29.45 (0.13)	0.498 (0.029)	0.682 (0.019)	99.74
MF13b	15	36.12 (1.36)	30.43 (0.7)	0.063 (0.009)	32.07 (0.55)	0.498 (0.044)	0.482 (0.02)	99.67
MF13c	14	36.23 (0.19)	30.31 (0.21)	0.009 (0.007)	32.18 (0.15)	0.648 (0.015)	0.328 (0.009)	99.71
MF14a	18	39.54 (0.2)	43.34 (0.27)	0.071 (0.01)	16.82 (0.34)	0.193 (0.012)	0.362 (0.03)	100.33
MF14b	19	39.14 (0.14)	40.57 (0.21)	0.05 (0.009)	21.1 (09.15)	0.236 (0.013)	0.083 (0.012)	101.18
MF15a	15	38.67 (0.13)	40.73 (0.1)	0.062 (0.009)	19.95 (0.15)	0.206 (0.01)	0.156 (0.009)	99.78
MF15b	15	38.97 (0.16)	41.48 (0.16)	0.042 (0.011)	19.11 (0.12)	0.201 (0.008)	0.224 (0.007)	100.03
MF15c	14	39.23 (0.24)	42.89 (0.19)	0.081 (0.005)	16.49 (0.08)	0.147 (0.005)	0.475 (0.009)	99.3
MF16a	16	32.77 (0.16)	43.64 (0.22)	0.095 (0.01)	22.99 (0.1)	0.263 (0.009)	0.139 (0.009)	99.98
MF16b	17	32.97 (0.15)	44.62 (0.16)	0.075 (0.006)	21.45 (0.09)	0.237 (0.007)	0.131 (0.009)	99.54
MF16c	17	39.35 (0.18)	43.13 (0.21)	0.089 (0.011)	17.54 (0.09)	0.221 (0.012)	0.326 (0.012)	100.7
MF17a	14	40.64 (0.15)	49.01 (0.12)	0.068 (0.007)	9.84 (0.04)	0.12 (0.008)	0.036 (0.006)	99.77
MF17b	14	40.49 (0.11)	48.42 (0.15)	0.064 (0.005)	10.85 (0.06)	0.088 (0.007)	0.032 (0.004)	99.99
MF17c	6	40.47 (0.14)	49.93 (0.10)	0.063 (0.006)	7.37 (0.05}	0.124 (0.006)	0.131 (0.005)	98.12

Notes:
[1]Value in parentheses is standard deviation of n analyses.
[2]The minimum detection limit for NiO is 0.011 wt% (99% confidence interval).

quenching is a technique that offers the most effective means of inhibiting quench crystallization of the melt (e.g., Kress, 1997), although the mineral–melt textural relations are obliterated by this process. Given that both sulfur and oxygen are the most fugitive components of the melt and that the quenching environment is characterized by large gradients in both fO_2 and fS_2, the anion chemistry of the sulfide liquid is judged to be most susceptible to modification. The most obvious evidence for quench modification of S and O is the formation of vesicles, which are present in experiments run without silicate melt (i.e., MF1ab and the D.ol series of Brenan and Caciagli, 2000) but largely absent from samples containing both melt types (see also Fig. 1). It may be that the loss of S and O from the sulfide melt in the latter experiments is reduced by the presence of the surrounding silicate melt, which acts as a barrier to volatile migration as a result of relatively slow diffusion of sulfur-bearing species (Watson, 1994). In any case, regular shifts in the anion content of sulfide liquids accompanied changes in imposed fS_2, fO_2, and melt Fe/Ni ratio, so relative changes in anion chemistry seem to be systematic, and probably reflect similar changes in the "prequench" compositions.

As previously observed by Gaetani and Grove (1999) and Rose and Brenan (2001), melt oxygen contents were found to increase with either fO_2 or melt Fe content. Figures 2A and 2B portray the molar O/O + S and oxygen content of melts for experiments performed at 1300°C and log fS_2 of -1.7 ± 0.1. For melts produced at log fO_2 of -10, the amount of dissolved oxygen is low, even for the most Fe-rich compositions. However, with increasing fO_2, the proportion of oxygen to sulfur rises, as does the total melt oxygen content, with the highest values of O/O + S and total oxygen measured for Fe-rich compositions produced at log fO_2 of -8.2 and -8.8. Replacement of Fe by Ni results in a decrease in melt O/O + S, and total oxygen levels, suggesting that oxygen dissolves in the melt as an Fe-oxide species. Like Ni, the addition of copper to the sulfide melt also resulted in a decrease in melt O/O + S and total oxygen content (Fig. 2C). Regardless of the identity of the "diluting" metal, melts with similar Fe contents have nearly the same proportion of oxygen to sulfur and oxygen concentrations (Fig. 2D), suggesting that Ni and Cu have similarly low affinities for oxygen in the sulfide melt.

3.3. Attainment of Equilibrium

Evidence for olivine–sulfide melt equilibrium is derived from two sets of observations. First, olivines produced in experiments are compositionally homogeneous, even after significant grain growth from the original starting material. This

Table 3. Summary of sulfide melt analyses (wt%)

Sample	n	O[1]	Fe	Ni	Cu	S	Total
MF1a	23	4.83 (0.81)	61.5 (1.08)	5.18 (1.24)	NA	28.71 (0.84)	100.23
MF1b	23	5.18 (0.93)	61.57 (1.25)	5.15 (1.18)	NA	28.4 (1.06)	100.31
MF2a	40	0.66 (0.63)	42.65 (2.39)	25.56 (2.82)	NA	30.87 (0.78)	99.74
MF2b	22	4.63 (0.81)	61.13 (0.74)	6.08 (0.84)	NA	28.2 (1.05)	100.04
MF3a	7	0 (0)	32.01 (1.96)	36.57 (2.57)	NA	30.54 (0.41)	99.11
MF3b	30	0.94 (1.51)	38.09 (3.24)	31.04 (3.86)	NA	29.58 (0.94)	99.66
MF4a	27	0.86 (0.75)	61.19 (0.35)	4.39 (0.34)	NA	33.45 (0.8)	99.9
MF4b	29	0 (0)	44.06 (1.7)	22.91 (2.14)	NA	32.49 (0.59)	99.46
MF5a	6	4.76 (1.31)	56.63 (1.4)	11.48 (1.44)	NA	27.24 (0.59)	100.1
MF5b	16	2.19 (1.02)	50 (2.54)	18.27 (2.92)	NA	28.49 (1.07)	98.95
MF6	19	0.06 (0.12)	52.64 (1.18)	13.75 (1.45)	NA	33.49 (0.54)	99.94
MF8a	20	0.16 (0.39)	52.51 (1.85)	13.33 (2.29)	NA	33.18 (0.81)	99.18
MF8b	15	0 (0)	44.84 (1.52)	21.87 (1.78)	NA	33.09 (0.34)	99.81
MF8c	20	0.5 (0.7)	59.28 (0.62)	5.93 (0.53)	NA	33.74 (0.68)	99.45
MF9a	25	1.56 (0.33)	50.21 (1.29)	16.35 (1.47)	NA	31.05 (0.35)	99.17
MF9b	14	4.79 (0.3)	61.57 (0.3)	5.46 (0.2)	NA	28.27 (0.35)	100.09
MF9c	16	0.23 (0.22)	41.98 (1.08)	24.96 (1.21)	NA	31.33 (0.33)	98.5
MF11a	5	4.25 (0.74)	57.01 (0.98)	10.8 (1.34)	NA	27.8 (0.47)	99.85
MF11b	20	3.61 (1.79)	49.95 (2.28)	18 (2.67)	NA	28.41 (1.11)	99.97
MF11c	18	2.53 (0.7)	40.59 (1.41)	28.34 (1.5)	NA	29.03 (0.48)	100.49
MF13a	20	0.47 (0.35)	38.45 (2.18)	29.39 (2.38)	NA	30.78 (0.29)	99.09
MF13b	17	2.27 (0.76)	47.82 (3.18)	19.23 (3.47)	NA	30 (0.57)	99.32
MF13c	18	6.13 (1.21)	59.64 (1.88)	7.81 (1.9)	NA	26.44 (1.19)	100.02
MF14a	14	0 (0)	42.2 (0.82)	24.34 (1.1)	NA	32.57 (0.4)	99.11
MF14b	11	2.93 (0.55)	60.02 (0.78)	5.36 (0.78)	NA	31.3 (0.61)	99.61
MF15a	20	5.01 (0.91)	60.74 (0.77)	5.28 (0.88)	NA	29.26 (0.86)	100.29
MF15b	17	3.47 (0.64)	54.92 (2.08)	11.63 (2.48)	NA	29.68 (0.54)	99.97
MF15c	18	0 (0)	35.98 (2.57)	32.14 (3.08)	NA	31.34 (0.69)	99.47
MF16a	13	3.02 (0.5)	52.99 (1.35)	7.39 (0.95)	6.74 (0.91)	29.2 (0.66)	99.33
MF16b	10	0.13 (0.14)	44.11 (1.42)	6.02 (0.49)	18.4 (1.55)	29.7 (0.5)	98.35
MF16c	15	0 (0)	35.4 (0.24)	17.27 (0.23)	16.31 (0.5)	30.17 (0.23)	99.15
MF17a	13	0.39 (0.34)	59.71 (0.23)	5.53 (0.34)	NA	33.92 (0.32)	99.54
MF17b	9	0.55 (0.28)	60.91 (0.23)	4.44 (0.34)	NA	33.68 (0.32)	99.58
MF17c	15	0.08 (0.16)	44.97 (1.94)	21.93 (2.44)	NA	32.4 (0.55)	99.38

Notes:
[1]Number in parentheses is standard deviation of n analyses.
NA = not added to experiment.

observation would suggest that dissolution/reprecipitation was the main mode of chemical exchange, which is far more efficient at achieving equilibrium than volume diffusion. Second, olivines produced by different synthesis "paths" yielded the same final K_D value. Experiments MF1a and 1b were two-stage experiments, each containing olivine and sulfide melt, with the latter using SCO and the former using forsterite oxide mix as starting materials. Samples were run for 4 d at $\log fO_2$ of -8.8, $\log fS_2$ of -1.7 and 1300°C. Upon quenching, each run product was extracted from its olivine crucible, finely powdered, packed into a fresh crucible, and rerun at the same conditions for an additional 4 d, so as to ensure complete chemical exchange. Measured values of K_D are identical for the two experiments (15.6 ± 4.8 and 13.8 ± 4.1; Table 1). In addition, a separate experiment (MF2b) was conducted under the same T-fO_2-fS_2 conditions as MF1a and 1b, but this time, the sample contained silicate melt (after the method of Fleet and MacRae, 1987) in addition to the sulfide melt and olivine. In this case, the experiment duration was 5 d, and the resulting olivine was significantly richer in FeO (22 wt%) and NiO (0.116 wt%) than the olivines from runs performed with just sulfide melt present (the latter olivines had ~11 wt% FeO and ~0.06 wt% NiO; Table 2). This large compositional contrast is a consequence of the higher abundance of FeO in the silicate melt–bearing experiment and of the resulting exchange of Ni for Fe in the olivine structure, by virtue of Eqn. 1. Despite the compositional difference, the resulting K_D value from this experiment (18.6 ± 2.8) is within error of values measured for the two-stage experiments (Table 1). In addition to reproducing the more arduous two-stage experiments, the silicate melt–bearing experiment also resulted in a more precise determination of K_D as a result of the higher FeO and NiO concentrations in run-product olivines. As will be shown below, most results from the experiments presented in this article are in very good accord with those originally published by Brenan and Caciagli (2000), although values of K_D from this latter work are more scattered and generally less precise, the result of lower Fe and Ni contents of run-product olivines.

Aside from MF1a and b, all other experiments performed in this study contained added silicate melt because its presence seems to enhance olivine–sulfide melt exchange. A 5-d run duration was determined to be sufficient for olivine–sulfide melt equilibrium, and with the exception of experiments MF15 and 17 (which were run at 1385°C for 3 d), all experiments were performed for this length of time. As a check on the approach to olivine-melt equilibrium for the 3-d experiments, some samples run for this duration (MF15b, MF17b) contained the forsterite oxide mix as a starting material. In the case of

MF17b, the value of K_D obtained (24.4 ± 4.0) is within error of the equivalent experiment using powdered SCO (25.3 ± 4.6; MF17a), a result that is consistent with equilibrium. The run product from experiment MF15b contained sulfide melt whose nickel content was shifted relative to the equivalent experiments that started with SCO. Given the dependence of K_D on melt Ni content (see below), such experiments were thus not directly comparable. However, results from those experiments all lie on the same K_D vs. wt% Ni correlation, regardless of starting material, suggesting equilibrium was achieved.

3.4. Variation in K_D with Melt Composition, fO_2, fS_2, and Temperature

Consistent with the previous results of Brenan and Caciagli (2000), values of K_D determined in this study showed systematic changes with both fO_2 and melt Fe/Ni ratio. As portrayed in Figure 3, K_D values for experiments run at log fO_2 of −8.1 to −8.8 were found to linearly increase with melt Ni concentration, and a comparison of the previous measurements of Brenan and Caciagli (2000) with values determined in this work shows excellent agreement over this fO_2 range. The extent of the melt composition effect appears to diminish with decreasing fO_2, however, because the slope of the K_D-wt% Ni variation lessens to zero at log $fO_2 \leq -9.5$ (Fig. 3C). The average K_D value for experiments performed at log fO_2 of −9.5 and −10 is ~31 (n = 6). This result is in contrast to that reported by Brenan and Caciagli (2000), in that the slope of the K_D-wt% Ni variation was interpreted to steepen with decreasing fO_2. Such an erroneous interpretation was largely based on data obtained from two experiments conducted at log fO_2 of −9.5, which contained ~5 wt% Ni in the sulfide melt. The resulting K_D values from those experiments are somewhat lower than those determined in this work, and those former values are of relatively poor precision, mainly because of the very low Ni content of run-product olivines. A summary diagram illustrating the relative shift in the K_D-wt% Ni correlation with fO_2 is provided in Figure 3D.

Although most experiments were performed at log fS_2 of −1.7, K_D was also determined at log fO_2 of −8.7, and log fS_2 of −0.9. Brenan and Caciagli (2000) also report results at similar fO_2, and log fS_2 of −4.1. Values of K_D determined at log fS_2 of −0.9 are essentially identical to those determined at log fO_2 of −8.8 and log fS_2 of −1.7 (Fig. 3B), indicating that K_D is insensitive to fS_2 over this range. In contrast, K_D determined in the high Ni experiment at log fS_2 of −4.1 is significantly displaced above the K_D-wt% Ni correlation defined by experiments performed at comparable fO_2, but higher fS_2.

The effect of temperature on K_D was assessed in experiments performed at 1200, 1300, 1385 and 1400°C and similar fS_2 conditions (Fig. 4). The K_D-wt% Ni correlation determined by Brenan and Caciagli (2000) at 1200°C, log fO_2 of −8.7 plots below that defined by data at log fO_2 of −8.8 at 1300°C (Fig. 4A), indicating that, at nearly constant fO_2, K_D values decrease with decreasing temperature. Consistent with this result are values of K_D determined at 1200°C and log fO_2 of −10, which are somewhat lower (22 to 26) than the average value of ~31 measured at 1300°C (Fig. 4B). In contrast to the data at 1200°C, for T ≥ 1300 and similar fO_2, the effect of T on K_D appears to be small. For example, the K_D measured by Brenan and Caciagli (2000) at 1400°C and log fO_2 of −8 with 28 wt% Ni in the sulfide melt is 24 ± 3, which is in very good agreement with the value of 23 predicted by the K_D-wt% Ni correlation determined for log fO_2 of −8.1 at 1300°C. Consistent with this result are data obtained in this study at 1385°C and log fO_2 of −8.5 and −8.9, which lie just below and above, respectively, the data for log fO_2 of −8.7 at 1300°C (Fig. 4C). An alternative way of assessing the T dependence of K_D is to consider how values change for the T-fO_2 conditions parallel to a solid oxide buffer, such as FMQ. This might be considered to be a more petrologically realistic evaluation of the temperature effect on K_D because natural magma suites appear to track parallel to the common solid oxide buffer curves (Carmichael, 1991). The experiments performed at log fO_2 of −9.1, 1200°C, and log fO_2 of −8.1, 1300°C are most appropriate for this comparison, as both oxygen fugacities correspond to ~0.8 log units more reducing than the FMQ buffer at those temperatures. In this case, values of K_D measured in the experiments performed at 1200°C are systematically larger than those measured at 1300°C (Fig. 4D), which is opposite to the temperature effect at constant fO_2.

Values of K_D measured by other workers involving experiments in which fO_2 and fS_2 were buffered are compared with data from this study in Figure 5. Boctor (1982) found that values of K_D increased from ~8 at an fO_2 of 10^{-8} to ~18 at an fO_2 of 10^{-9} for experiments conducted at 1300 to 1400°C in which the sulfide liquid contained 1 to 9.6 wt% nickel (Fig. 5A). The magnitude of this increase is generally consistent with the K_D-wt% Ni correlations determined in this study, as melt with low Ni contents showed more than a two-fold increase in K_D as fO_2 decreased from $\sim 10^{-8}$ to $\sim 10^{-9}$. Figure 5B shows the K_D-wt% Ni correlation from experiments performed at log fO_2 of ~8, 1300 to 1350°C and log fS_2 of −1.1 to −2.5. The data of Gaetani and Grove (1997) plot on the high Ni extrapolation of the results of this study, as do some of the data from Fleet and MacRae (1988). However, at melt Ni contents of 20 to 30 wt%, K_D values of Fleet and MacRae (1988) are somewhat higher than those measured in this study. Other values of K_D measured by Gaetani and Grove (1997) at 1350°C and log fO_2 of −9.4 and −10.3 are in good agreement with those measured in this study at 1300°C, with the exception of a single, exceptionally high value (~46) determined at log fO_2 of −10.3 (Fig. 5C).

Figure 5D shows the results of experiments performed by Fleet and MacRae (1987) at 1385°C, log fS_2 of −1 and log fO_2 of −8.7 compared with those of this study performed at identical T and fS_2, and log fO_2 of −8.5 and −8.9. The latter results show a positive correlation between K_D and wt% Ni whose slope lessens with decreasing fO_2. In contrast, the data of Fleet and MacRae (1987) show values of K_D that are uniformly higher than those determined in this study, and that are essentially invariant with melt Ni content (averaging ~35). The discrepancy is puzzling, given that both this study and that of Fleet and MacRae (1987) employed similar experimental techniques, including the addition of silicate melt, and tests for reversal that involved the use of different olivine compositions in the starting material. The only difference in experiment design is the use of alumina crucibles in the Fleet and MacRae (1987) study, in contrast to olivine used in the current work. Similar results to Fleet and MacRae (1987) were obtained in

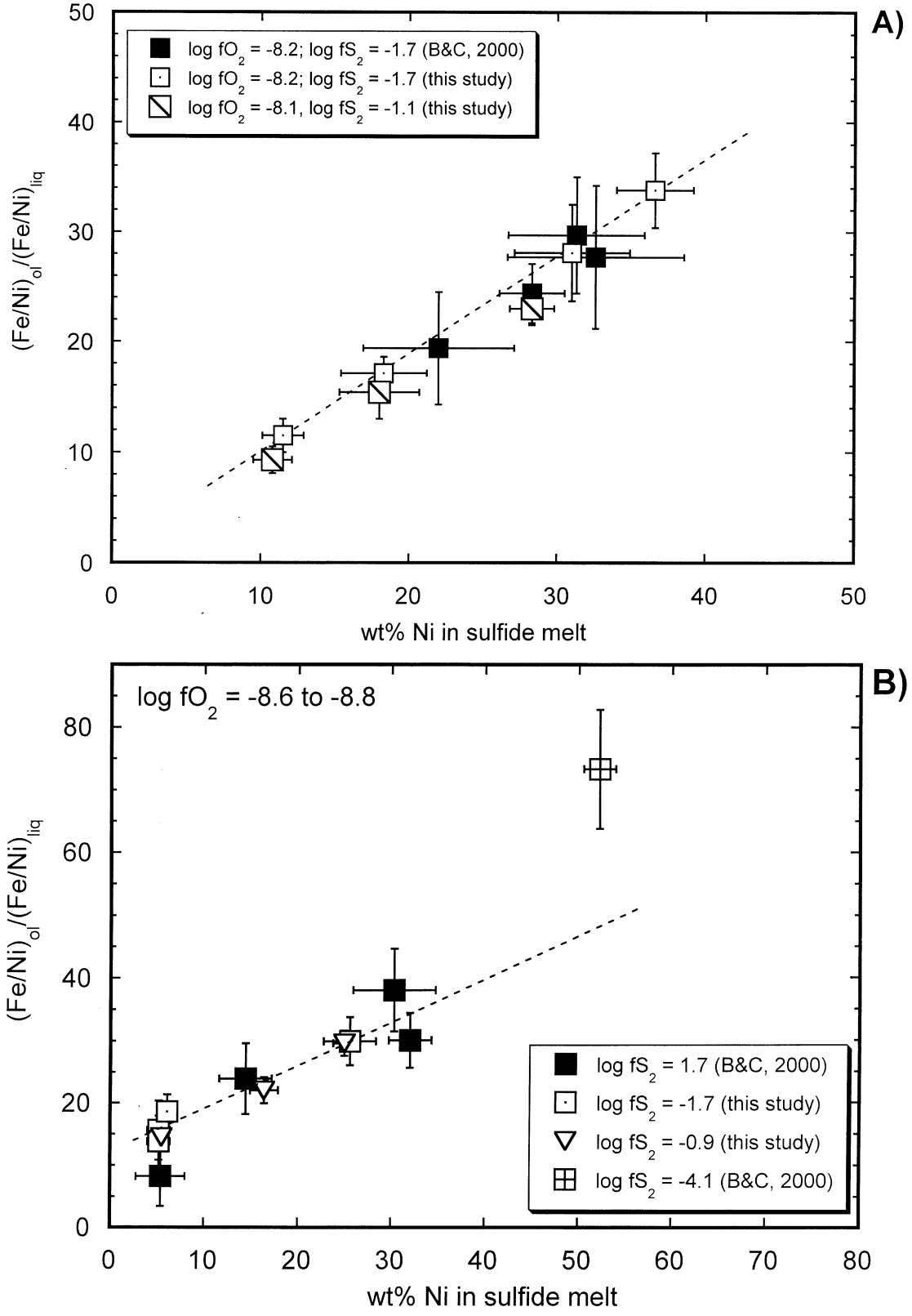

Fig. 3. Variation in olivine-melt Fe-Ni exchange coefficient (K_D) as a function of wt% Ni in the sulfide liquid. Data are shown for experiments conducted at log fS_2 of −0.9 to −4.1, temperature of 1300°C, log fO_2 of (A) −8.1 and −8.2, (B) −8.8, and (C) −9.5 and −10. Values of K_D are plotted for all forward experiments from Brenan and Caciagli (2000) and the new results from this study. Dashed curves in all diagrams were determined by linear regression of the new data by the method of York (1969). The data portrayed in (D) are a summary of the results from this study for experiments performed at 1300°C, log fS_2 of −1.7 ± 0.1.

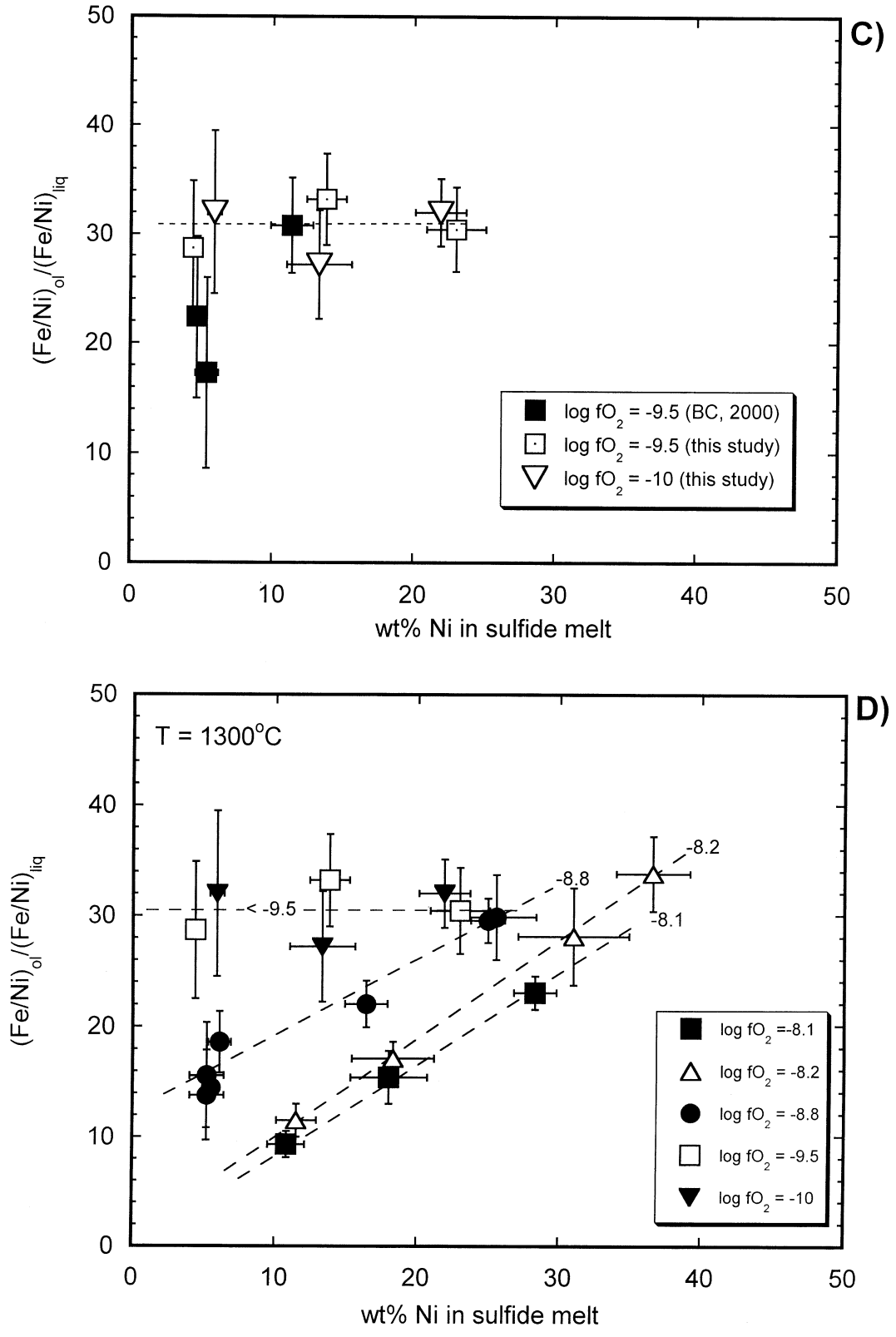

Fig. 3. (Continued)

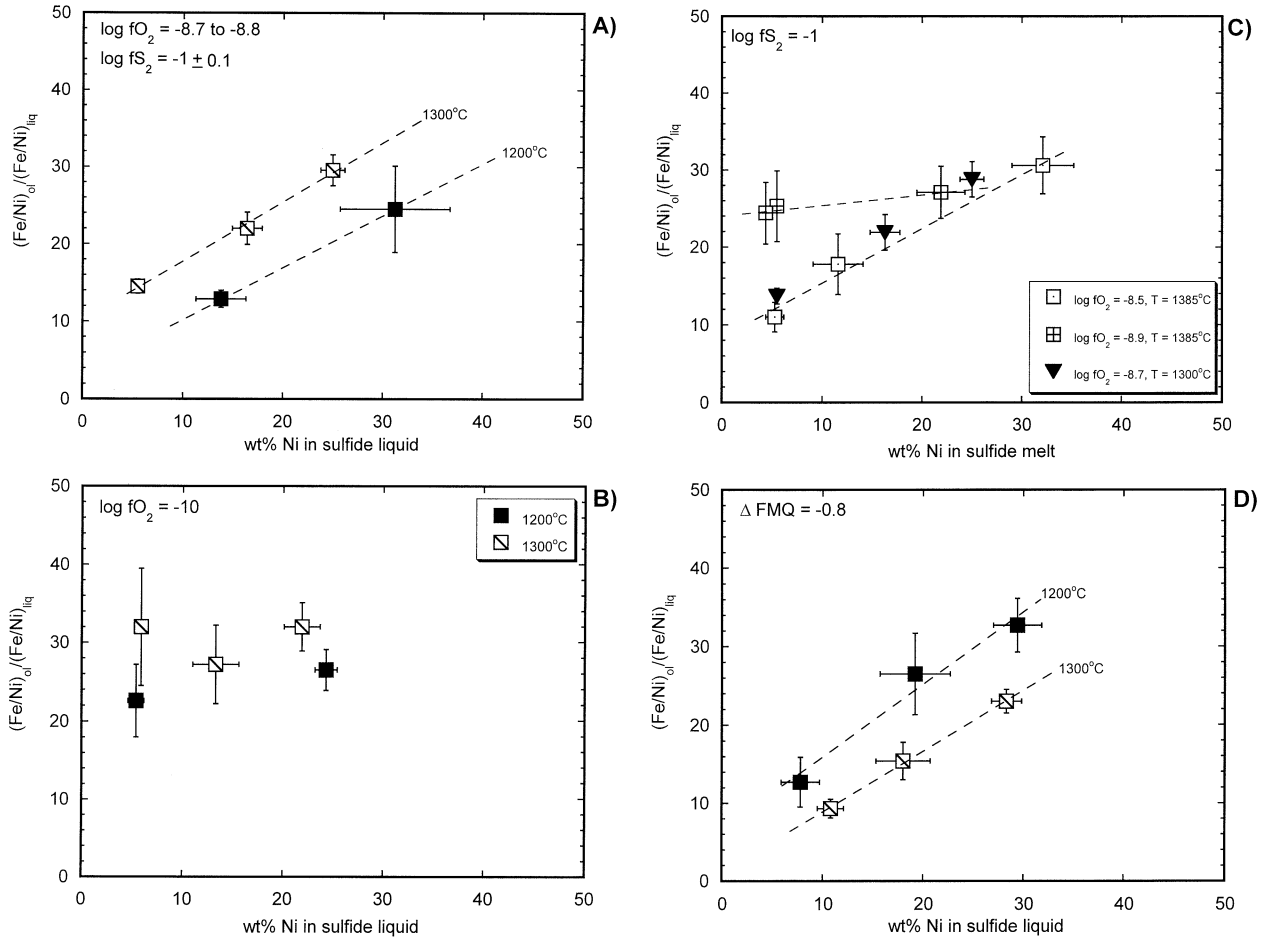

Fig. 4. (A–C) Comparison of K_D values determined at different temperatures but nearly constant fO_2 and fS_2. (D) Effect of temperature if the fO_2 changes at a constant value of 0.8 log units more reduced than the FMQ buffer.

this study at log fO_2 values ~0.8 log units more reducing (i.e., lower than −9.5) at 1300°C (Fig. 3C). Given that K_D values seem to be relatively insensitive to temperature above 1300°C, it seems likely that a constant K_D should be encountered at similarly low fO_2 at 1385°C. Indeed, the small slope of the K_D-wt% Ni correlation determined at log fO_2 of −8.9 at 1385°C appears to support this prediction (Fig. 5D). Thus, it is possible that the origin of the discrepancy between the results of this study and that of Fleet and MacRae (1987) is that there is a systematic offset in the reported value of furnace fO_2. Specifically, it is suggested that the actual furnace fO_2 of Fleet and MacRae's experiments is lower than in this study by ~0.8 log units (or possibly less, given that K_D becomes constant between log fO_2 of −8.8 and −9.5 at 1300°C). In terms of the overall accuracy of furnace fO_2, the values reported in this study have been confirmed by replicating solid oxide buffer reactions and "sliding" redox sensors, and on this basis are accurate to within 0.3 log units (see Experimental and Analytical Methods). The experimental work reported by Fleet and MacRae (1987, 1988) does not include any evaluation of fO_2 accuracy, but if it is similar to that reported in this study, then the aforementioned difference seems permissible.

Values of K_D for Cu-doped experiments from this study and Gaetani and Grove (1997) are portrayed as a function of the Cu + Ni content of the sulfide melt in Figure 6. The reason for the use of the sum of Ni + Cu as the melt compositional parameter is because of the similar effects of these elements on controlling the oxygen content of the sulfide melt; Ni and Cu are simply dilutants for the major oxide species in the melt, Fe, as shown in Figures 2C and D. As will be discussed in the following section on the variation in K_D with melt composition, the oxygen content of the sulfide melt appears to exert an overwhelming control on this behavior. As shown in Figure 6, K_D values for sulfide melt having the lowest Cu content (~7 wt%) are consistent with the K_D-wt% Ni correlations determined from Cu-free experiments. Experiments containing higher Cu contents are, however, displaced to the right of those curves, yielding K_D values that are lower than expected.

3.5. Origin of the Variation in K_D with Melt Composition

As previously discussed by Brenan and Caciagli (2000), the dependence of K_D on melt composition reflects nonideal mixing behavior of one or more of the species involved in the olivine-melt Fe-Ni exchange reaction. With respect to olivine, Hirschmann (1991) has shown that mixing in ternary Mg-Fe-Ni olivines can be viewed as nearly ideal, provided temperature is high, the olivine is magnesium-rich ($>Fo_{80}$) and the mole

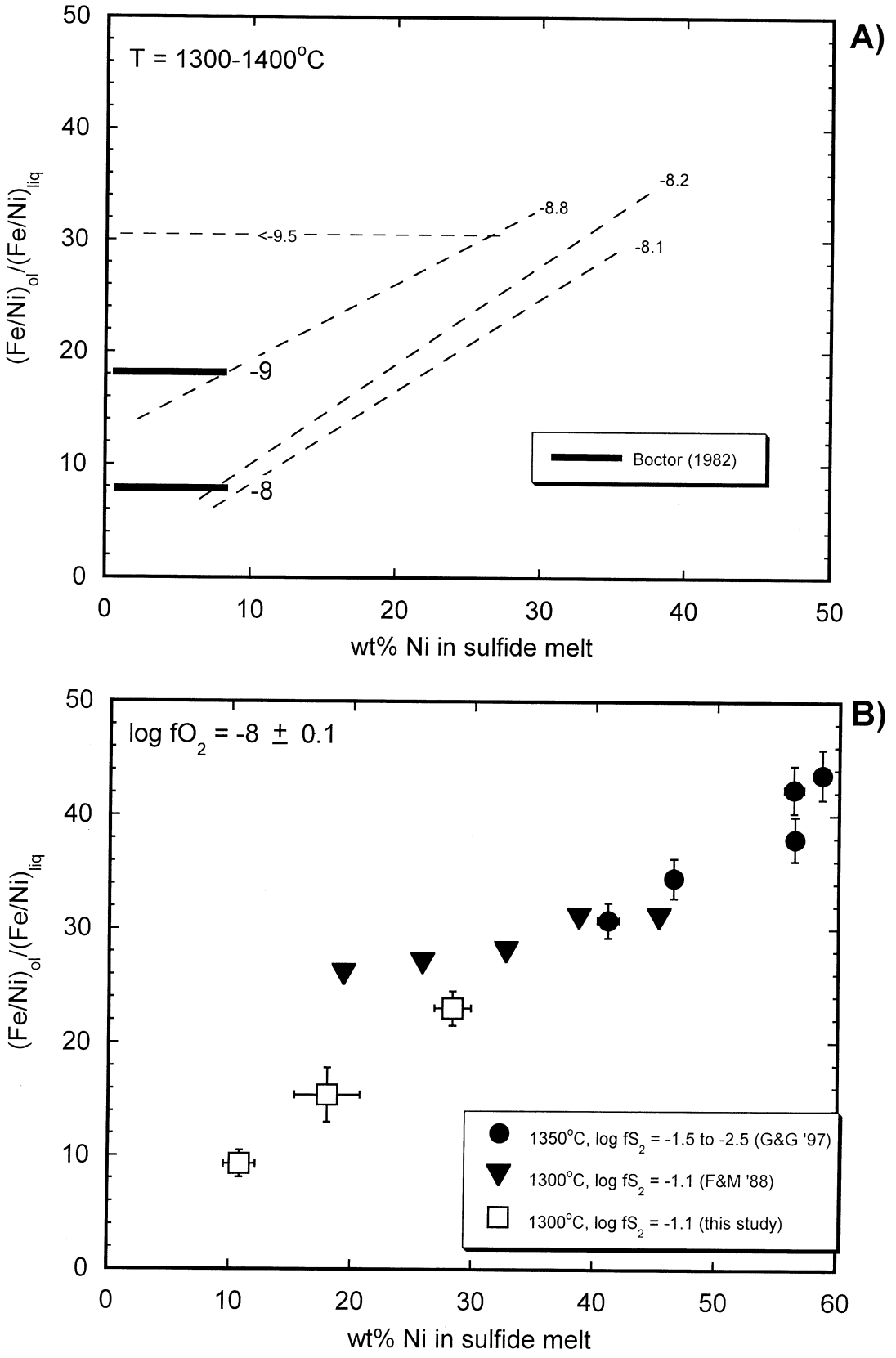

Fig. 5. Comparison of K_D values from this study with those determined previously. Data are from Boctor (1982), Gaetani and Grove (1997), and Fleet and MacRae (1987, 1988). The horizontal bars in (A) portray the average K_D value reported by Boctor (1982) for melts with 1 to 9.6 wt% Ni performed at 1300 to 1400°C and the log fO_2 indicated. In (A), the dashed curves are the best-fit lines for the K_D-wt% Ni correlations from Figure 3D.

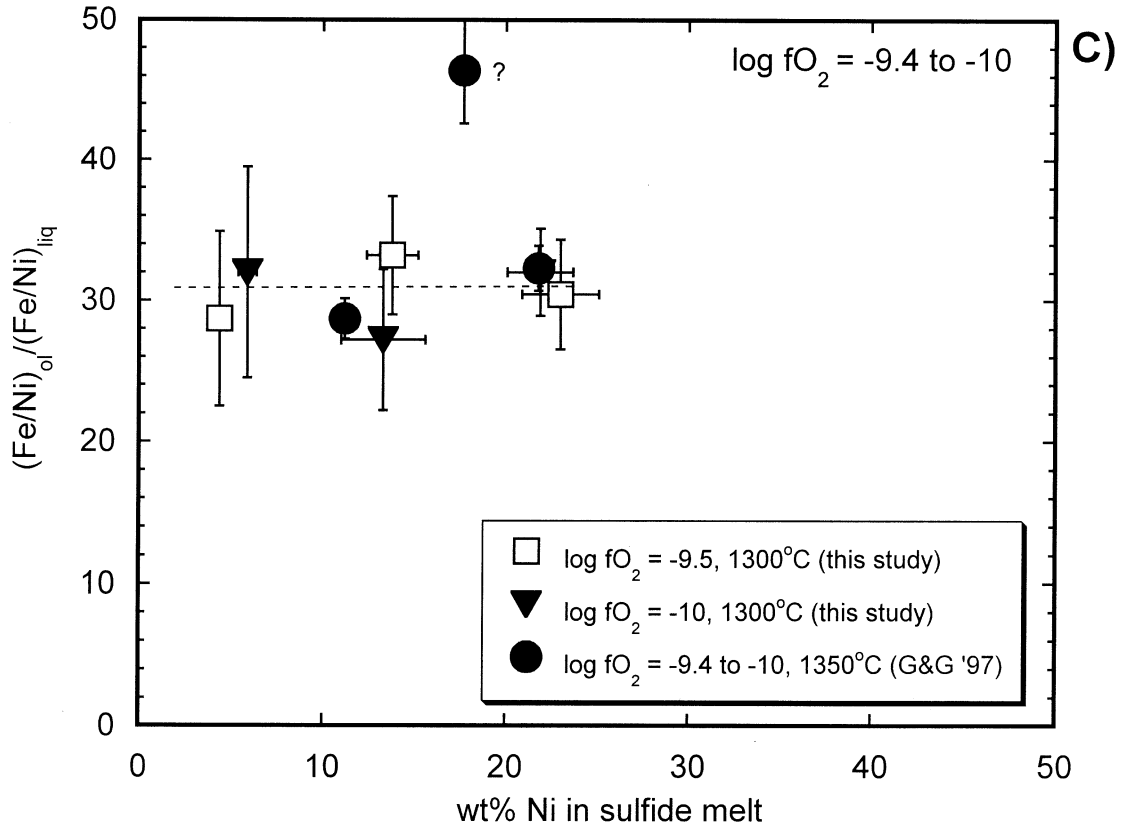

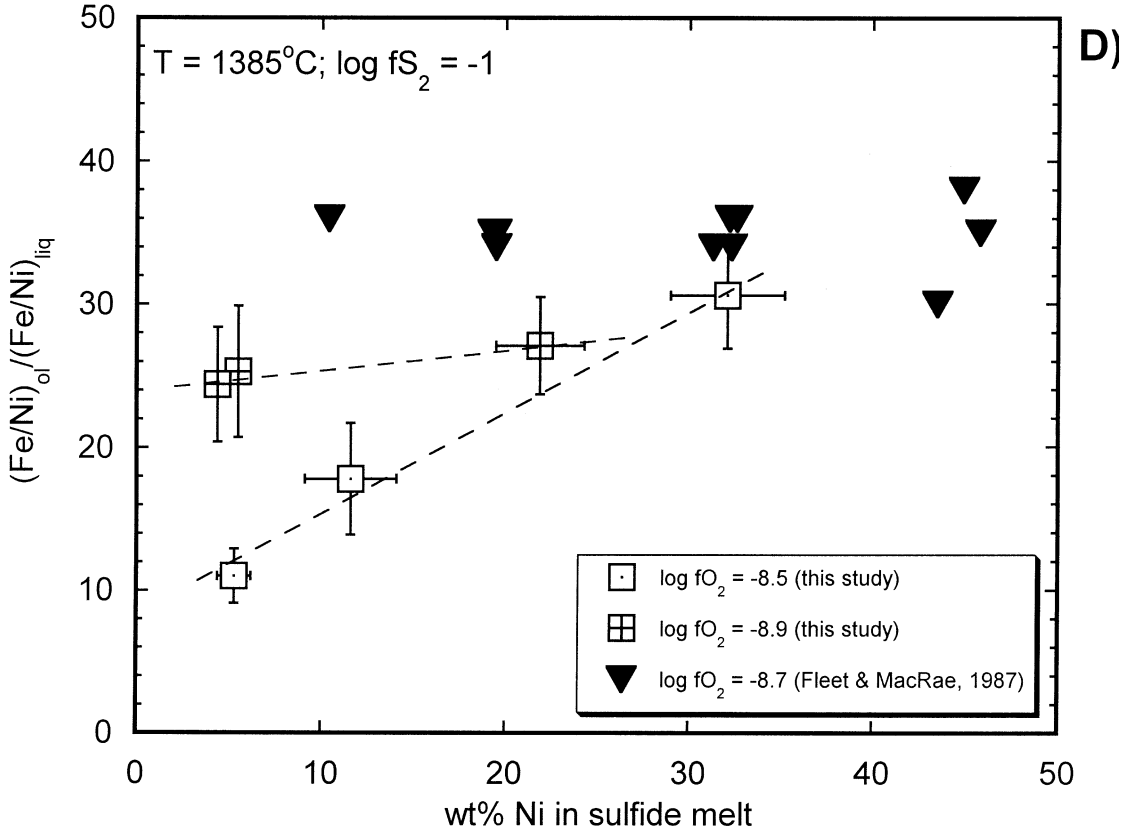

Fig. 5. (Continued)

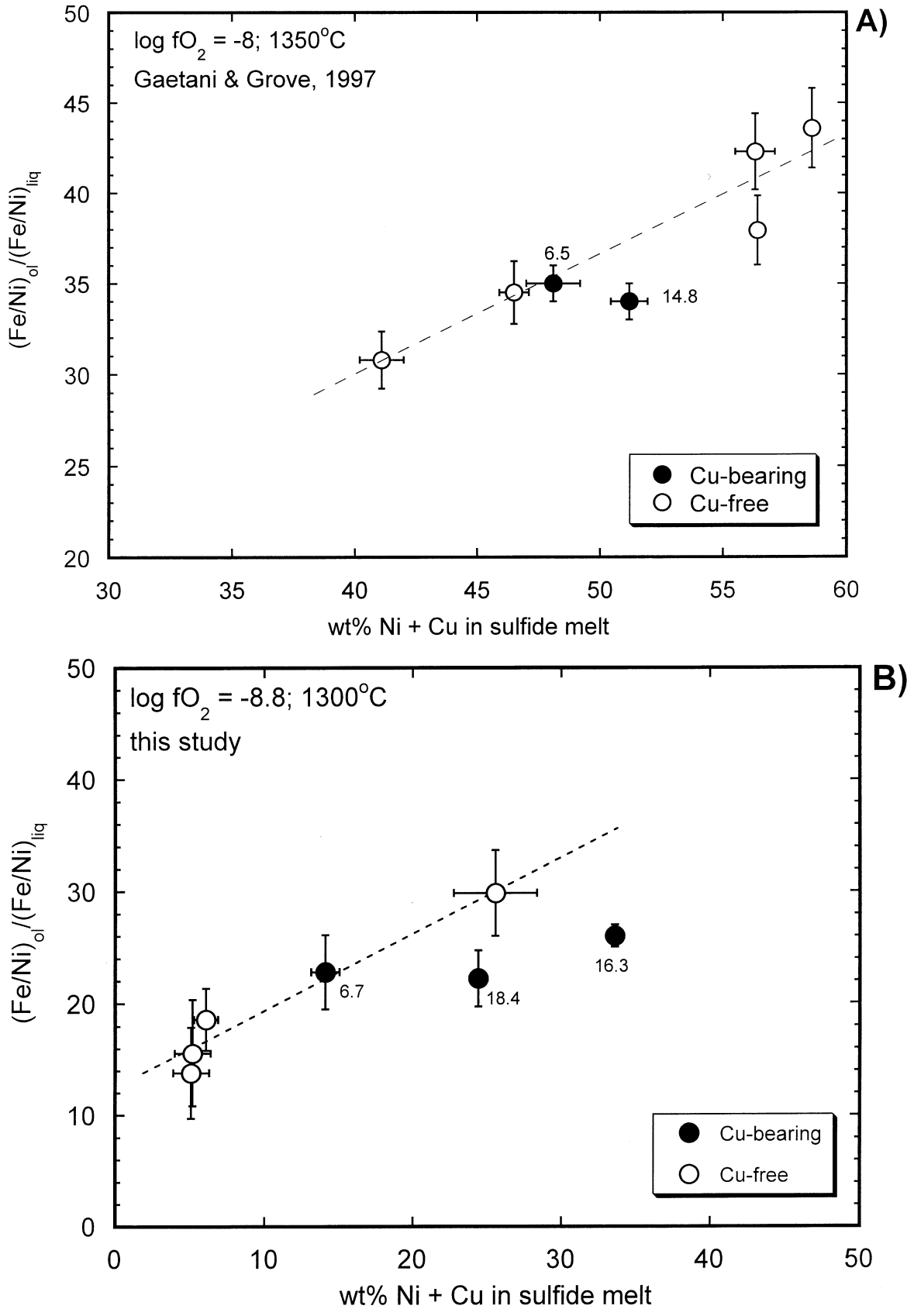

Fig. 6. Comparison of K_D values determined from experiments performed with Cu-bearing and Cu-free sulfide liquids. Data from this study and Gaetani and Grove (1997) Labels on data points correspond to wt% Cu in the sulfide liquid.

fraction of the $NiSi_{½}O_2$ component is small; requisites that are largely met in the experiments of this study. In support of this contention are similar K_D values measured in experiments containing olivines with very different Fe contents (i.e., MF1a, b and MF2b). It thus seems likely that the dominant contribution to the variation in K_D is from nonideal mixing in the sulfide liquid. Doyle and Naldrett (1987) showed that for Fe-S-O melts having $X_{Fe} > 0.49$, mixing of oxide and sulfide species is nonideal, with activity coefficients varying with melt O/O + S. These workers hypothesized that similar nonideal behavior should exist for mixing of other metal species, like Ni, and that if the activity coefficients for FeS and NiS (γ_{FeS}, γ_{NiS}, respectively) do not vary in the same way with melt oxygen content, then K_D will not be constant. In light of this analysis, the observed variation of K_D with melt Ni content in high fO_2 experiments likely reflects the sympathetic change in melt oxygen content arising from the role of Ni (± Cu) as a dilutant for Fe, which is the major oxide species in the melt (e.g., Figs. 2A–D). Consistent with this interpretation, the data portrayed in Figure 7A show a clear correlation between K_D and the molar O/O + S of the sulfide melt for all experiments performed at 1300°C. By virtue of Eqn. 2, the overall reduction in K_D with melt O/O + S requires an increase in γ_{NiS} relative to γ_{FeS}, and hence a decrease in X_{NiS}/X_{FeS} to maintain the same activity ratio, thereby implying nonideal mixing in the sulfide melt. It is notable that the amount of dissolved oxygen in the sulfide melt required to lower K_D values to within the range of many magmatic sulfide ores (i.e., ~10) is ~5 wt%, which corresponds to ~20 wt% magnetite in the fully crystallized melt. This amount is about half the value originally estimated by Doyle and Naldrett (1987), based on "guesstimates" of the oxygen content of sulfide liquids produced by Boctor (1981, 1982). Although most sulfide ores contain 10 wt% or less magnetite, the amount of oxygen required to be "lost" by reaction with the silicate magma is much less than Doyle and Naldrett (1987) previously suggested.

The constant K_D value of ~31 in experiments performed at $\log fO_2$ of ≤ -9.5 indicates that the relative values of γ_{NiS} and γ_{FeS} in such oxygen-poor melts must be invariant over the range in melt Fe/Ni ratio investigated. However, nonideal mixing behavior is well documented in oxygen-poor, metal-rich sulfide melts, and it is anticipated that values of K_D may differ significantly from 31 as a result of this effect. For example, studies of binary Fe-S, Ni-S and ternary Fe-Ni-S and Fe-*S*-O melts (Nagamori et al., 1969; Nagamori and Ingraham, 1970; Hsieh et al., 1987; Kress, 1997) indicate that, for sulfur-rich compositions, the activity coefficients for Fe- and Ni-sulfide species decrease with increased metal/sulfur ratio, and the decrease is larger for Ni than for Fe species. Moreover, the data of Ebel and Naldrett (1996) show that the equilibrium constant for MSS-liquid Fe-Ni exchange increases as a function of melt metal/sulfur ratio, provided this latter ratio is greater than ~0.95 (Fig. 7B). Given that activity-composition relations for MSS are largely ideal (cf. data summarized in Naldrett, 1989), those results verify that there is a larger decrease in γ_{NiS} than for γ_{FeS} with increasing melt metal/sulfur, and predicts that the olivine–sulfide melt K_D for Fe-Ni exchange should increase accordingly. The relatively constant K_D value measured in experiments performed at $\log fO_2$ of ≤ -9.5 is therefore likely to be a consequence of the limited range in metal/sulfur of the melts produced in those experiments (1.10 to 1.16). In contrast, the shift in K_D accompanying a much larger change in metal/sulfur for experiments performed at $\log fO_2$ of -8.7 ± 0.1 is shown in Figure 7C. In this case, only experiments that produced oxygen-poor sulfide liquids (O/O + S < 0.05) are portrayed. The very large K_D value measured in the experiment performed at $\log fS_2$ of -4.1 is consistent with the preceding predictions, given the high metal/sulfur ratio (1.6) in the sulfide liquid. It might therefore be anticipated that natural metal-rich sulfide liquids produced at low sulfur fugacities would yield K_D values >30, as illustrated by that result.

3.6. Application to Natural Olivine–Sulfide Assemblages

Previously, Brenan and Caciagli (2000) used the systematic variation in K_D with fO_2 and melt Ni content to derive an expression for estimating fO_2 in natural olivine + sulfide-bearing assemblages. In that original formulation, the slopes of fO_2 isopleths in K_D-wt% Ni space were interpreted to increase with decreasing fO_2, and the limiting value of K_D was assumed to be near zero for Ni-free compositions. The more precise data obtained in the current study would suggest that, although there is a marked reduction in K_D with fO_2 and melt Ni content, these relations are more complex than originally thought. Specifically, the new data indicates that the slope of the K_D-wt% Ni relationship actually lessens with decreasing fO_2, and the limiting value of K_D for Ni-free compositions increases. It was also previously assumed that T, fS_2 and the addition of Cu to the sulfide melt all had minimal effects on K_D, and although these assumptions are still largely correct, the limits over which these effects are minor are now better determined.

Armed with the combined data sets of this study and that of Brenan and Caciagli (2000), a reappraisal of Brenan and Caciagli's original interpretation of the origin of the variation in K_D values from natural olivine–sulfide assemblages can be made. In this case, a data suite similar to that used by Brenan and Caciagli (2000) is compared here, with the exception that only assemblages containing low-Cu (<7 wt%) sulfide melt compositions are considered. This exclusion is made because the results of this study show that only melts with less than ~7 wt% Cu adhere to the K_D-wt% Ni + Cu variation determined at a specific fO_2 by using Ni-free compositions. In addition, any sulfide-bearing occurrences that have undergone alteration (i.e., the Dumont deposit; Thompson et al., 1984) or metamorphism (Perseverance, Renzy Lake, Great Lakes Nickel; Fleet and MacRae, 1983), are excluded from this analysis, as a result of the possibility of recrystallization and subsolidus exchange. For each sample, K_D values are calculated from data obtained by EMP analyses of olivine combined with sulfide liquid compositions determined by reconstituting the subsolidus sulfide assemblage by using either bulk analyses or by combining individual sulfide phase analyses with their modal proportions. The reader is referred to the specific references on each suite for more detailed compositional information (see caption to Fig. 8).

Values of K_D as a function of the nickel + copper content of the reconstituted sulfide liquid are portrayed in Figure 8, and included in this diagram are contours of K_D vs. wt% Ni + Cu measured in this study at 1300°C and $\log fS_2$ of -0.9 to -1.7. As has been recognized for some time, relatively large varia-

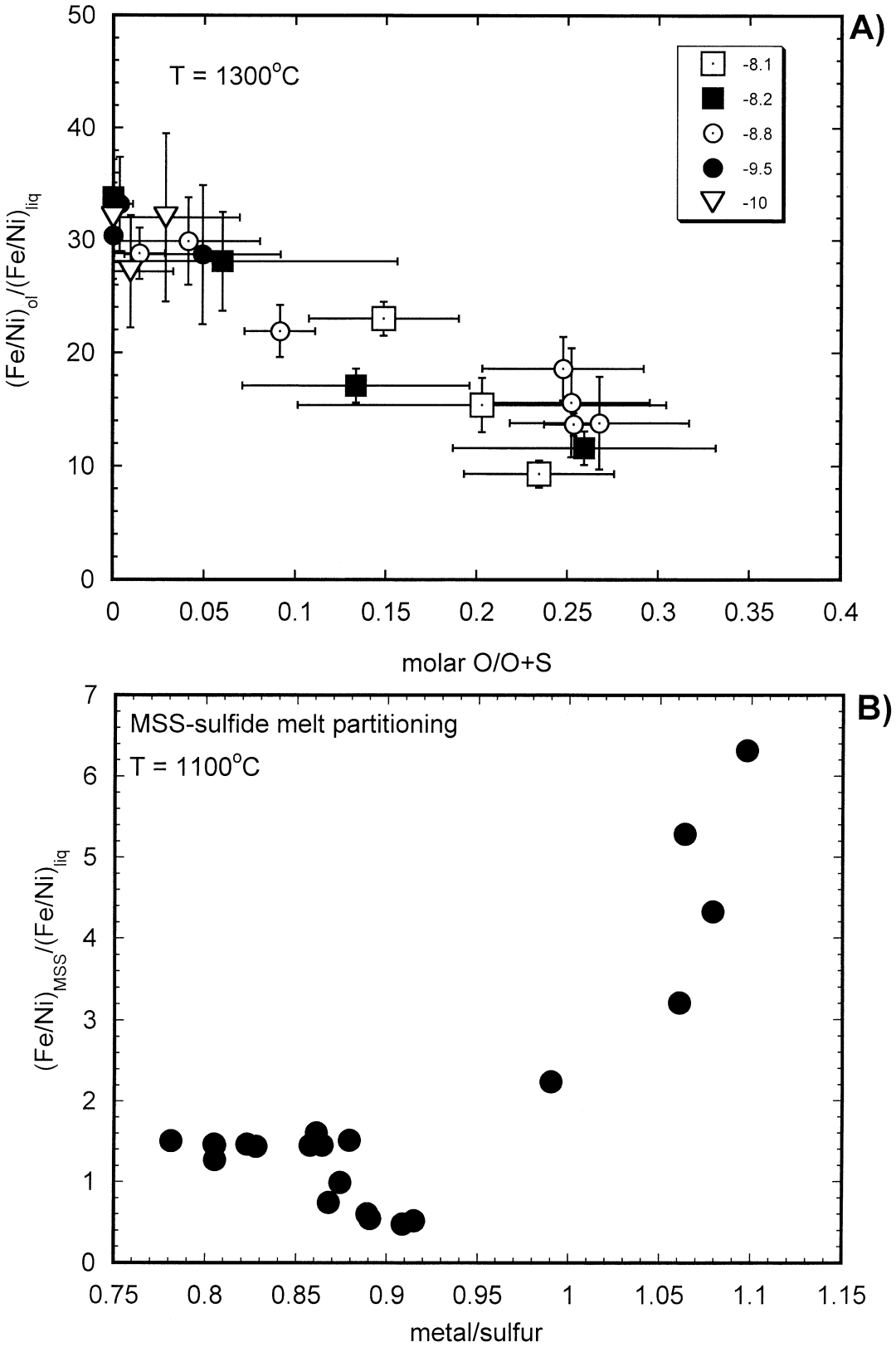

Fig. 7. Evaluation of the effect of the anion content of sulfide melt on K_D. (A) K_D as a function of the molar O/O + S ratio of sulfide melt from experiments performed at 1300°C, log fS_2 of −0.9 to −1.7 and the log fO_2 values indicated. (B) Variation in the Fe-Ni exchange coefficient between monosulfide solid solution (MSS) and sulfide melt as a function of the metal/sulfur ratio of the sulfide melt. Note the abrupt rise in the value of the exchange coefficient when the metal/anion ratio exceeds ~0.95. Data from Ebel and Naldrett (1996).

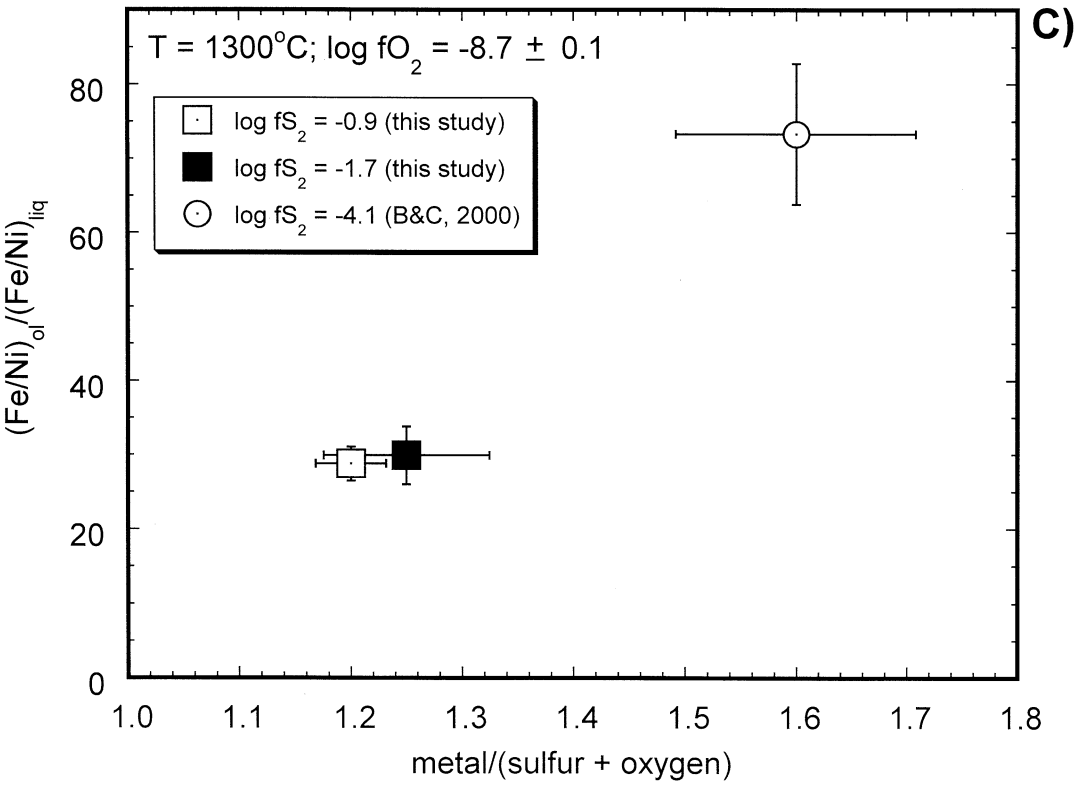

Fig. 7. (Continued) (C) K_D as a function of the molar metal/anion (S + O) ratio for experiments with O/O + S less than 0.05, performed at the log fS_2 indicated, and log fO_2 of -8.7 ± 0.1.

tions exist in K_D values from these different rock suites, and where multiple determinations have been made, K_D values from a single suite also show significant differences. Brenan and Caciagli's original interpretation was that the observed differences exhibited by the natural suites is a consequence of the variation in K_D with melt nickel content and fO_2, with the suites that exhibit relatively low values of K_D (<20) and moderate nickel contents (5 to 20 wt%) arising from olivine–sulfide liquid equilibrium under relatively oxidizing conditions. Conversely, they suggested that low nickel suites with high values of K_D formed under relatively reducing conditions. Comparison of the experimental results of this study with the natural data indicates that their original interpretation was generally robust. However, given the misinterpretation of their experimental data as discussed above, Brenan and Caciagli's estimates of fO_2 for natural samples are inaccurate, despite a favorable comparison between their results and fO_2 estimates from other sources. Reasonably accurate estimates of fO_2 from natural K_D data can be made by using the results of this study, however, provided the fS_2 of natural samples does not vary significantly from the range of $\sim 10^{-1}$ to $\sim 10^{-2}$. Sulfur fugacity estimates for sulfide liquid-saturated oceanic lavas (Wallace and Carmichael, 1992) suggests this prerequisite is generally met. As shown in Figure 8, the observed variation in natural K_D values is consistent with fO_2 ranging from $\sim 10^{-8.2}$ (FMQ-1 at 1300°C) to $10^{-9.5}$, or lower (FMQ-2 at 1300°C). Given that quenching temperatures for samples in the volcanic suite are ~1200°C or less (see Brenan and Li, 2000), estimated fO_2 will be lower than the 1300°C values on the basis of the effect of temperature on the K_D-wt% Ni correlation at constant fO_2 determined in this study. However, because the absolute fO_2 of the FMQ buffer decreases with temperature, the relative difference in sample fO_2 with respect to FMQ may be similar to the 1300°C estimate. Such estimates of fO_2 are in very good agreement with values determined for oceanic basalts by using glass ferric/ferrous ratios (e.g., Christie et al., 1986; Carmichael, 1991; Wallace and Carmichael, 1992).

Although most values of K_D from natural olivine–sulfide assemblages are within the range that have been reproduced experimentally, the data set from volcanic suites shows a few values that are anomalously high for their respective melt Ni contents. Specifically, two tephra samples from Kilauea contain olivine–sulfide pairs containing 35 to 40 wt% Ni in the sulfide with K_D values of 40 to 55, and a sample from Disko Island with 5 wt% Ni in the sulfide yielded a K_D of ~70. Although olivine–sulfide disequilibrium is certainly one possible explanation for these results, it is also possible that the fS_2 at which those samples formed was lower than the range over which the experiments of this study were performed (i.e., $\sim 10^{-1}$ to $\sim 10^{-2}$). Given the high K_D value determined by Brenan and Caciagli (2000) for a sample equilibrated at log fS_2 of -4.1, combined with the previous prediction of the effect of lowering fS_2 on increasing melt metal/sulfur, and hence raising K_D, this interpretation seems reasonable. Moreover, for the case of the Disko Island sample, there are various indicators that this sample crystallized at an unusually low fO_2 ($\sim 10^{-14}$ or FMQ-5.7 at 1200°C), including the presence of native iron, and samples that yielded exceptionally large olivine–melt partition

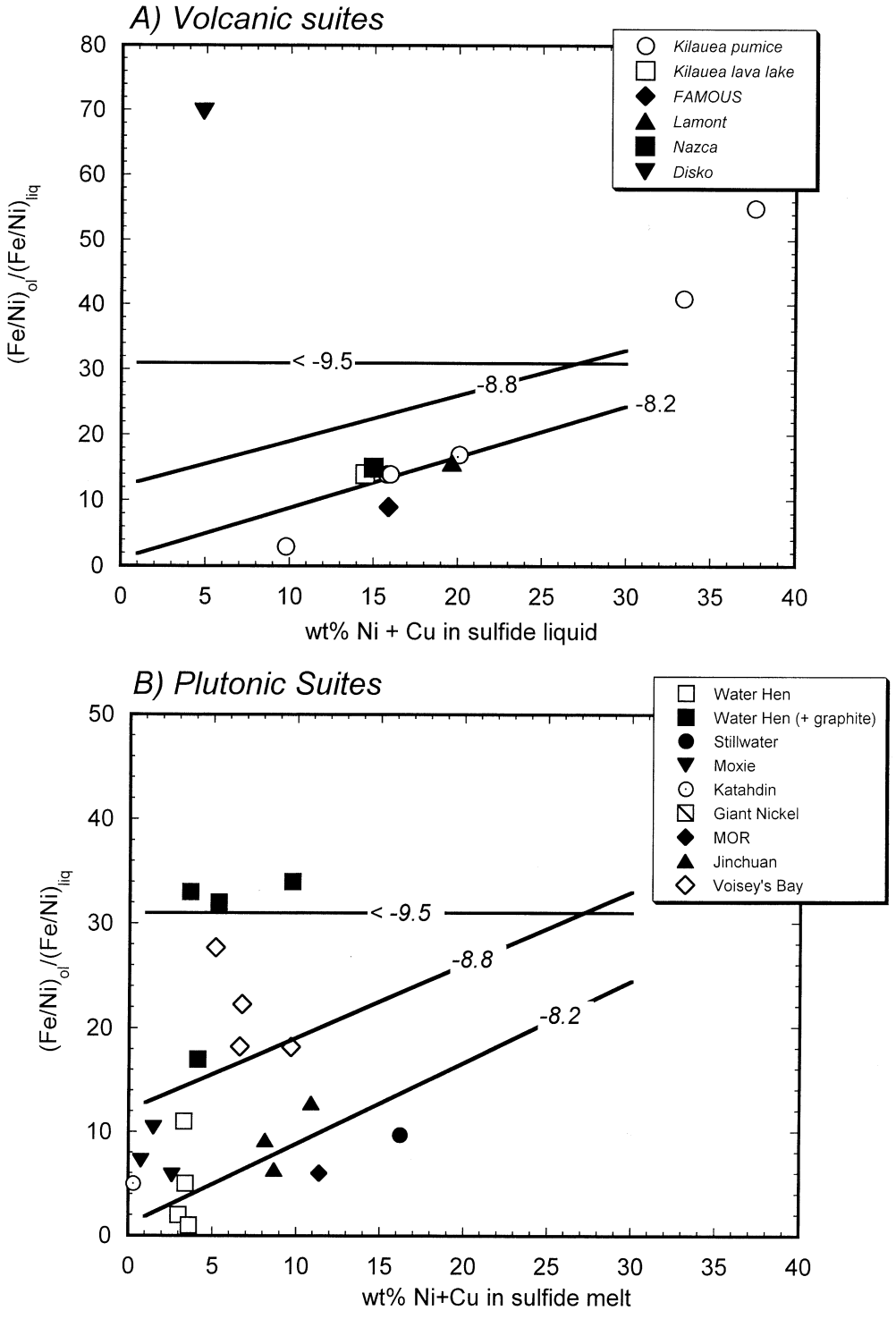

Fig. 8. K_D as a function of wt% nickel + copper in the sulfide liquid for olivine + sulfide-saturated volcanic (A) and plutonic (B) suites. Curves, labeled in terms of corresponding log fO_2, are the linear regression of experiments performed in this study at 1300°C, log fS_2 of −0.9 to −1.7. Data are portrayed only for samples containing sulfide melt compositions with less then 7 wt% copper. Data for Kilauea correspond to tephra and lava lake samples produced in the 1959 subaerial eruption; FAMOUS (volcanic), Nazca and Lamont are ocean floor basalts; Disko is a native iron-bearing Tertiary subvolcanic mafic dike from Disko Island, west Greenland; Water Hen is the Water Hen intrusion in the Duluth Complex; Stillwater is from the J-M reef of the Stillwater complex; Moxie and Katahdin are mafic/ultramafic intrusions in northwest Maine, USA; Giant Nickel is an ultramafic intrusion in western British Columbia, Canada; MOR (plutonic) are peridotite and gabbro in Leg 37 drill core from the FAMOUS area; Jinchuan is an ultramafic dike in Gansu, northwest China; Voiseys's Bay is a troctolite body in central Labrador, Canada. Data sources are as follows: Kilauea, FAMOUS, Nazca (references in Fleet and Stone, 1990); Lamont (Allen et al., 1989; J. Allen, personal communication); Disko (Pederson, 1979); Water Hen (Mainwaring, 1976); Stillwater (Barnes and Naldrett, 1985); Moxie, Katahdin (Thompson et al., 1984); Giant Nickel (Muir, 1971); Jinchuan (Chai and Naldrett, 1992a,b); and Voisey's Bay (Brenan and Li, 2000).

coefficients for vanadium and chromium (see Brenan and Caciagli, 2000). Inasmuch as the fS_2 required for sulfide liquid saturation in a silicate magma decreases with fO_2 (e.g., Wallace and Carmichael, 1992), the low values of fO_2 recorded by the sulfide-saturated Disko Island lavas imply correspondingly low fS_2 during crystallization.

As a final point to this discussion, Brenan and Caciagli (2000) noted that the oxygen fugacities they estimated for sulfide-saturated mafic and ultramafic intrusive rocks were significantly more variable than the extrusive data set, with nearly equal numbers of samples exhibiting oxidation states similar to oceanic basalts as those showing a more reduced character. Although the absolute values of fO_2 they inferred for those suites are inaccurate, the relative variation in fO_2 both within and between suites is supported by the results of the experiments presented in this study. These relations are also clearly evident in Figure 8. The origin of this variation is discussed by Brenan and Caciagli (2000) and Brenan and Li (2000), the latter authors noting that the most persistent feature of the low fO_2 samples from the intrusive suites is evidence for assimilation of locally exposed carbonaceous and sulfidic rock units. The overall reduced nature of such suites could be attributed to reaction of an initially oxidized magma with graphite during the assimilation process, with reduction occurring by the reaction (Holloway et al., 1992)

$$C_{graphite} + 2\,Fe_2O_{3\,melt} + O^{2-}{}_{melt} = CO_3{}^{2-}{}_{melt} + 4FeO_{melt} \quad (3)$$

in which $O^{2-}{}_{melt}$ refers to available bridging or nonbridging oxygen in the silicate melt and $CO_3{}^{2-}{}_{melt}$ refers to CO_2 dissolved as the carbonate species (Brey and Green, 1976; Mysen et al., 1976; Fine and Stolper, 1986). It is notable that several samples from the intrusive suite are saturated in graphite (Disko, Water Hen, Voisey's Bay), and within the Water Hen and Voisey's Bay intrusions, graphite-bearing samples have generally lower fO_2s than their graphite-free counterparts (Fig. 8B; see also Brenan and Li, 2000), thus supporting the graphite assimilation hypothesis.

4. CONCLUSIONS

Measurements of the apparent equilibrium constant (K_D) for the exchange of Fe and Ni between coexisting olivine and sulfide liquid have shown its dependence, to varying extent, on melt composition, fO_2, fS_2 and temperature. As originally documented by Brenan and Caciagli (2000), values of K_D were found to increase with the nickel content of the sulfide liquid, although the current data set shows this dependence is greatest at log fO_2 of -8.1, lessens with decreasing fO_2, and K_D becomes independent of melt Ni content at log $fO_2 \leq -9.5$. At log fO_2 of -8.7 ± 0.1 and log fS_2 of -0.9 to -1.7, K_D was found to be relatively insensitive to sulfur fugacity, whereas at log fS_2 of -4.1, a much higher value of K_D was measured. The variation in K_D with fO_2 and fS_2 most likely stems from changes in $\gamma_{NiS}/\gamma_{FeS}$ with either melt oxygen content or metal/sulfur ratio, which is the result of nonideal mixing in the sulfide liquid. Application of these results to interpreting natural samples reveals that the relatively large variations that exist in K_D values from different olivine + sulfide–saturated rock suites can be reconciled by variations in fO_2 and/or the nickel content of the sulfide liquid. This interpretation is also consistent with the findings of Brenan and Caciagli (2000). Counter to the conclusions of Fleet and coworkers (Fleet and MacRae, 1983; Fleet and Stone, 1990), the low values of K_D measured in samples from several intrusive and extrusive rock suites do not necessarily reflect disequilibrium but are in fact, consistent with olivine–sulfide equilibrium within the T-fS_2-fO_2 range experienced by terrestrial magmas.

Acknowledgments—This work was supported by the Natural Sciences and Engineering Research Council of Canada. Reviews by Glenn Gaetani, Wim van Westrenen, an anonymous referee, and A. E. Bjorn Mysen were most helpful for improving the quality and clarity of the manuscript. I am grateful to Dave Andrews for his help in design and fabrication of sample holders, and Natalie Caciagli provided useful comments on an earlier version of this article. Mike Fleet is thanked for pointing out some inconsistencies in the original Brenan-Caciagli data interpretation, which led to this latest round of experiments.

Associate editor: B. Mysen

REFERENCES

Allen J. F., Batiza R., Perfit M. R., Fornari D. J., and Sack R. O. (1989) Petrology of lavas from the Lamont seamount chain and the adjacent East Pacific Rise. *J. Petrol.* **30,** 1245–1298.

Andrews D. A., and Brenan J. M. (2002) The solubility of ruthenium in sulfide liquid: Implications for platinum-group mineral (PGM) stability and sulfide melt/silicate melt partitioning. *Chem. Geol.*, **192,** 163–181.

Barnes S. J. and Naldrett A. J. (1985) Geochemistry of the J-M (Howland) Reef of the Stillwater complex, Minneapolis Adit area. I. Sulfide chemistry and sulfide–olivine equilibrium. *Econ. Geol.* **50,** 627–645.

Boctor N. Z. (1981) Partitioning of nickel between olivine and iron monosulfide melts. Annual Report of the Director, Geophysical Laboratory, Carnegie Institute, Washington, **80,** 356–359.

Boctor N. Z. (1982) The effect of fO_2, fS_2 and temperature on Ni partitioning between olivine and iron sulfide melt. Annual Report of the Director, Geophysical Laboratory, Carnegie Institute, Washington, **81,** 366–369.

Brenan J. M. and Caciagli N. C. (2000) Fe-Ni exchange between olivine and sulphide liquid: Implications for oxygen barometry in sulphide-saturated magmas. *Geochim. Cosmochim. Acta* **64,** 307–320.

Brenan J. M. and Li C. (2000) Constraints on oxygen fugacity during sulfide segregation in the Voisey's Bay intrusion, Labrador, Canada. *Econ. Geol.* **95,** 901–915.

Brey G. P. and Green D. H. (1976) Solubility of CO_2 in olivine melilitite at high pressures and the role of CO_2 in the Earth's upper mantle. *Contrib. Mineral. Petrol.* **55,** 217–230.

Carmichael I. S. E. (1991) The redox state of basic and silicic magmas: A reflection of their source regions? *Contrib. Mineral. Petrol.* **106,** 129–141.

Chai G. and Naldrett A. J. (1992a) Characteristics of Ni-Cu-PGE mineralization and genesis of the Jinchuan deposit, northwest China. *Econ. Geol.* **87,** 1475–1495.

Chai G. and Naldrett A. J. (1992b) The Jinchuan ultramafic intrusion: Cumulate of a high-Mg basaltic magma. *J. Petrol.* **33,** 277–303.

Christie D. M., Carmichael I. S. E., and Langmuir C. H. (1986) Oxidation states of mid-ocean ridge basalt glasses. *Earth Planet. Sci. Lett.* **79,** 397–411.

Clark T. and Naldrett A. J. (1972) The distribution of Fe and Ni between synthetic olivine and sulfide at 900°C. *Econ. Geol.* **67,** 939–952.

Doyle C. D. and Naldrett A. J. (1987) The oxygen content of "sulfide" magma and its effect on the partitioning of nickel between coexisting olivine and molten ores. *Econ. Geol.* **82,** 208–211.

Ebel D. S. and Naldrett A. J. (1996) Fractional crystallization of sulfide ore liquids at high temperature. *Econ. Geol.* **91,** 607–621.

Fine G. J. and Stolper E. M. (1986) Dissolved carbon dioxide in basaltic glasses: Concentrations and speciation. *Earth Planet. Sci. Lett.* **76,** 263–278.

Fleet M. E. (2001) A comment on "Fe-Ni exchange between olivine and sulphide liquid: Implications for oxygen barometry in sulphide-saturated magmas" by Brenan and Caciagli (2000). *Geochim. Cosmochim. Acta* **65,** 4425–4427.

Fleet M. E., MacRae N. D., and Herzberg C. T. (1977) Partition of nickel between olivine and sulfide: A test for immiscible sulfide liquids. *Contrib. Mineral. Petrol.* **65,** 191–197.

Fleet M. E., MacRae N. D., and Osborne M. D. (1981) The partition of nickel between olivine, magma and immiscible sulfide liquid. *Chem. Geol.* **32,** 119–127.

Fleet M. E. and MacRae N. D. (1983) Partition of Ni between olivine and sulfide and its application to Ni-Cu sulfide deposits. *Contrib. Mineral. Petrol.* **83,** 75–81.

Fleet M. E. and MacRae N. D. (1987) Partition of Ni between olivine and sulfide: The effect of temperature, fO_2 and fS_2. *Contrib. Mineral. Petrol.* **95,** 336–342.

Fleet M. E. and MacRae N. D. (1988) Partition of Ni between olivine and sulfide: Equilibria with sulfide-oxide liquids. *Contrib. Mineral. Petrol.* **100,** 462–469.

Fleet M. E. and Stone W. E. (1990) Nickeliferous sulfides in xenoliths, olivine megacrysts and basaltic glass. *Contrib. Mineral. Petrol.* **105,** 629–636.

Gaetani G. A. and Grove T. L. (1997) Partitioning of moderately siderophile elements among olivine, silicate melt and sulfide melt: Constraints on core formation in the Earth and Mars. *Geochim. Cosmochim. Acta* **61,** 1829–1846.

Gaetani G. A. and Grove T. L. (1999) Wetting of mantle olivine by sulfide melt: Implications for Re/Os ratios in mantle peridotite and late-stage core formation. *Earth Planet. Sci. Lett.* **169,** 147–163.

Hirschmann M. (1991) Thermodynamics of multicomponent olivines and the solution properties for (Ni, Mg, Fe)$_2$SiO$_4$ and (Ca, Mg, Fe)$_2$SiO$_4$ olivines. *Am. Mineral.* **76,** 1232–1248.

Holloway J. R., Pan V., and Gudmundsson G. (1992) High pressure fluid-absent melting experiments in the presence of graphite: Oxygen fugacity, ferric/ferrous ratio and dissolved CO_2. *Eur. J. Mineral.* **4,** 105–114.

Hsieh K.-C., Vlach K. C., and Chang Y. A. (1987) The Fe-Ni-S system I. A thermodynamic analysis of the phase equilibria and calculation of the phase diagram from 1173 to 1623 K. *High Temperature Sci.* **23,** 17–38.

Kress V. (1997) Thermochemistry of sulfide liquids. I. The system O-S-Fe at 1 bar. *Contrib. Mineral. Petrol.* **127,** 176–186.

Mainwaring P. R. (1976) The petrology of a sulfide-bearing layered intrusion at the base of the Duluth Complex, St. Louis County, Minnesota. Ph.D. thesis. University of Toronto.

Muir J. E. (1971) A study of the "4600" ore body at the Giant Nickel Mine, Hope, B.C. Ph.D. thesis. University of Toronto.

Mysen B. O., Eggler D. H., Seitz M. G., and Holloway J. R. (1976) Carbon dioxide solubilities in silicate melts and crystals. Part 1. Solubility measurements. *Am. J. Sci.* **276,** 455–479.

Nagamori M., Hatakeyama T., and Kameda M. (1969) Thermodynamics of the iron-sulfur melts in the temperature range of 1100°–1300°C. *J. Jpn. Inst. Metals* **33,** 366–370.

Nagamori M. and Ingraham T. R. (1970) Thermodynamic properties of Ni-S melts between 700°C and 1100°C. *Metall. Trans.* **1,** 1821–1825.

Naldrett A. J. (1989) *Magmatic Sulfide Deposits.* Oxford Monographs on Geology and Geophysics No. 14. Oxford University Press.

Peach C. L. and Mathez E. A. (1993) Sulfide melt-silicate melt distribution coefficients for nickel and iron and implications for the distribution of other chalcophile elements. *Geochim. Cosmichim. Acta* **57,** 3013–3021.

Pederson A. K. (1979) Basaltic glass with high-temperature equilibrated immiscible sulphide bodies with native iron from Disko, central west Greenland. *Contrib. Mineral. Petrol.* **69,** 397–407.

Pownceby M. I. and O'Neill H. St. C. (1994) Thermodynamic data from redox reactions at high temperatures. III. Activity-composition relations in Ni-Pd alloys from EMF measurements at 850–1250 K, and calibration of the NiO + Ni-Pd assemblage as a redox sensor. *Contrib. Mineral. Petrol* **116,** 327–339.

Roeder P. L. and Reynolds I. (1991) Crystallization of chromite and chromium solubility in basaltic melts. *J. Petrol.* **32,** 909–934.

Rose L. A. and Brenan J. M. (2001) Wetting properties of Fe-Ni-Co-Cu-O-S melts against olivine: Implications for sulfide melt mobility. *Econ. Geol.* **96,** 145–157.

Thompson J. F. H. (1982) The intrusion and crystallization of mafic magmas, central Maine, and genesis of their associated sulfides. Ph.D. thesis. University of Toronto.

Thompson J. F. H., Barnes S. J., and Duke J. M. (1984) The distribution of nickel and iron between olivine and magmatic sulfides in some natural assmblages. *Can. Min.* **22,** 55–66.

Toulmin P. III and Barton P. B. Jr (1964) A thermodynamic study of pyrite and pyrrhotite. *Geochim. Cosmochim. Acta* **28,** 641–671.

York D. (1969) Least squares fitting of a straight line with correlated errors. *Earth Planet. Sci. Lett.* **5,** 320–324.

Wallace P. and Carmichael I. S. E. (1992) Sulfur in basaltic magmas. *Geochim. Cosmochim. Acta* **56,** 1863–1874.

Watson E. B. (1994) Diffusion in volatile-bearing magmas. In *Volatiles in Magmas* (eds. M. R. Carroll and J. R. Holloway), pp. 371–412. Mineralogical Society of America Reviews in Mineralogy 30.